The Astrophysics of Ultrahigh-Energy Cosmic Rays

Kumiko Kotera and Angela V. Olinto

Department of Astronomy and Astrophysics, Kavli Institute for Cosmological Physics, The University of Chicago, Chicago, Illinois 60637; email: kotera@uchicago.edu, olinto@kicp.uchicago.edu

Annu. Rev. Astron. Astrophys. 2011. 49:119–53

First published online as a Review in Advance on May 19, 2011

The *Annual Review of Astronomy and Astrophysics* is online at astro.annualreviews.org

This article's doi:
10.1146/annurev-astro-081710-102620

0066-4146/11/0922-0119$20.00

Keywords

active galaxies, compact objects, cosmic accelerators, cosmic background radiation, gamma-ray bursts, gamma rays, magnetic fields, neutrinos, particle astrophysics

Abstract

The origin of the highest energy cosmic rays is still unknown. The discovery of their sources is expected to reveal the workings of the most energetic astrophysical accelerators in the Universe. Current observations show a spectrum consistent with an origin in extragalactic astrophysical sources. Candidate sources range from the birth of compact objects to explosions related to gamma-ray bursts or to events in active galaxies. We discuss the main effects of propagation from cosmologically distant sources, including interactions with cosmic background radiation and magnetic fields. We examine possible acceleration mechanisms leading to a survey of candidate sources and their signatures. New questions arise from an observed hint of sky anisotropies and an unexpected evolution of composition indicators. Future observations may reach the necessary sensitivity to achieve charged particle astronomy and to observe ultrahigh-energy photons and neutrinos, which may further illuminate the workings of the Universe at these extreme energies. In addition to fostering a new understanding of high-energy astrophysical phenomena, the study of ultrahigh-energy cosmic rays can constrain the structure of the Galactic and extragalactic magnetic fields as well as probe particle interactions at energies orders of magnitude higher than achieved in terrestrial accelerators.

1. INTRODUCTION

The observation that cosmic rays can exceed 10^{20} eV poses some interesting and challenging questions: Where do they come from? How can they be accelerated to such high energies? What kind of particles are they? What is the spatial distribution of their sources? What do they tell us about these extreme cosmic accelerators? How strong are the magnetic fields that they traverse on their way to Earth? How do they interact with the cosmic background radiation? What secondary particles are produced from these interactions? What can we learn about particle interactions at these otherwise inaccessible energies? Here, we review recent progress toward answering these questions.

The dominant component of cosmic rays observed on Earth originates in the Galaxy. As shown in **Figure 1**, the study of this striking nonthermal spectrum requires a large number of instruments to cover over 8 orders of magnitude in energy and 24 orders of magnitude in flux. Galactic cosmic rays are likely to originate in supernova remnants (see, e.g., Hillas 2006, for a recent update on the origin of Galactic cosmic rays). A transition from Galactic to extragalactic cosmic rays should occur somewhere between 1 PeV ($\equiv 10^{15}$ eV) and 1 EeV ($\equiv 10^{18}$ eV). Progress on determining this

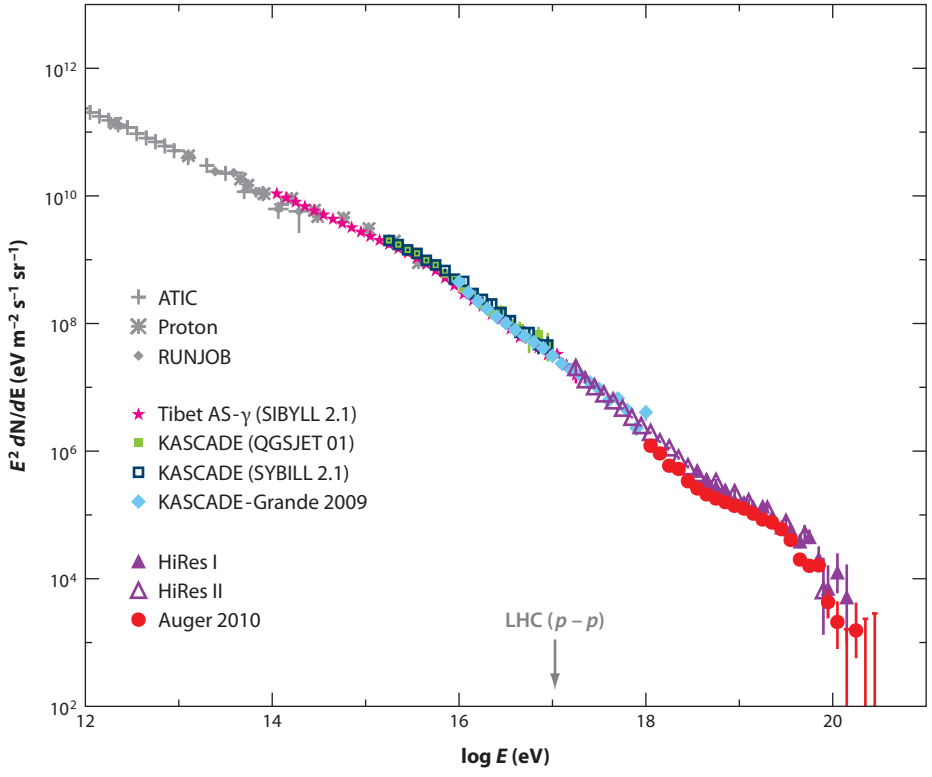

Figure 1

All particle cosmic ray flux multiplied by E^2 observed by ATIC (Advanced Thin Ionization Calorimeter; Ahn et al. 2008), Proton (Grigorov et al. 1971), RUNJOB (Russian Nippon Joint Balloon experiment; Apanasenko et al. 2001), Tibet AS-γ (Tibet Air-Shower Gamma Experiment, Amenomori et al. 2008), KASCADE (Karlsruhe Shower Core and Array Detector; Kampert et al. 2004), KASCADE-Grande (Karlsruhe Shower Core and Array Detector-Grande; Apel et al. 2009), HiRes I (High Resolution Fly's Eye I; Abbasi et al. 2009), HiRes II (High Resolution Fly's Eye II, Abbasi et al. 2008b), and Auger (the Pierre Auger Observatory; Abraham et al. 2010b). Large Hadron Collider (LHC) energy reach of $p - p$ collisions (in the frame of a proton) is indicated for comparison.

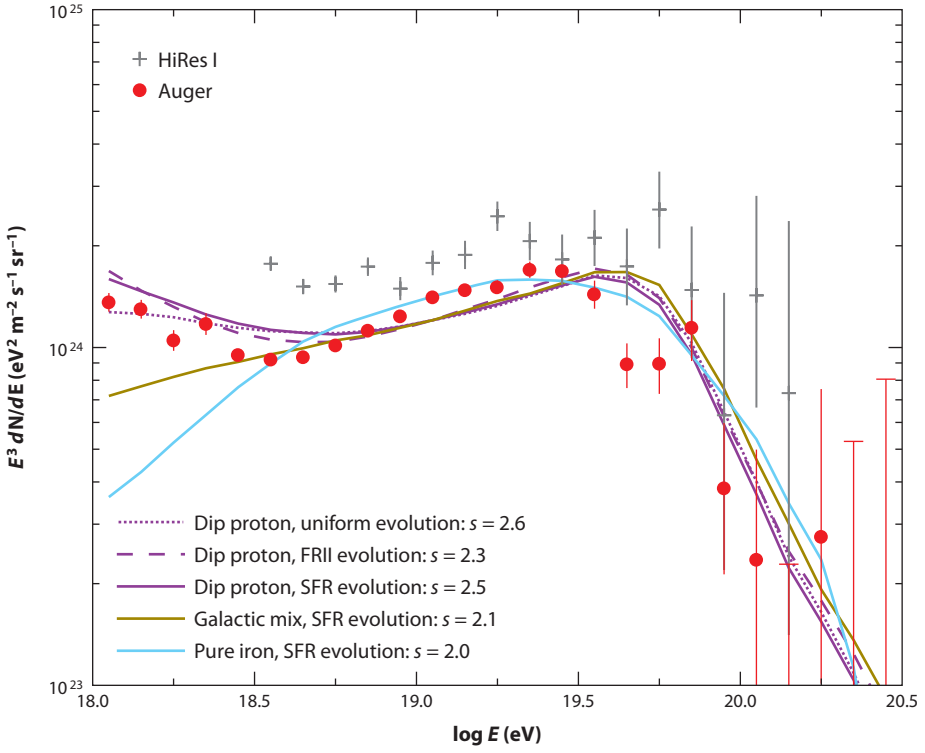

Figure 2

Spectrum of ultrahigh-energy cosmic rays multiplied by E^3 observed by HiRes I (High Resolution Fly's Eye; Abbasi et al. 2009) and Auger (the Pierre Auger Observatory; Abraham et al. 2010b). Overlaid are simulated spectra obtained for different models of the Galactic to extragalactic transition and different injected chemical compositions and spectral indices, *s*, described in Sections 2.1 and 4.

transition relies both on the study of the highest energies reached in Galactic accelerators as well as the search for extragalactic accelerators that produce ultrahigh-energy cosmic rays (UHECRs).

We begin with a brief summary of recent observations (Section 2), which reveal a spectrum whose shape supports the long-held notion that sources of UHECRs are extragalactic. As shown in **Figure 2**, the crucial spectral feature recently established at the highest energies is a steep decline in flux above about 30 EeV. This feature is reminiscent of the effect of interactions between extragalactic cosmic rays and the cosmic background radiation, named the Greisen-Zatsepin-Kuzmin (GZK) cutoff (Greisen 1966, Zatsepin & Kuzmin 1966). Another important feature shown in **Figure 2** is the hardening of the spectrum at around 4 EeV, called the ankle, which may be caused by the transition from Galactic to extragalactic cosmic rays or by propagation losses if UHECRs are mostly protons.

As discussed in Section 2, recent reports of a trend toward a heavier composition from around 4 EeV up to 40 EeV together with hints of anisotropies in the sky distribution above 60 EeV raise new and unexpected puzzles. An anisotropic sky distribution is expected for trans-GZK energies (i.e., energies above 60 EeV) if UHECRs are mainly protons, due to a combination of (*a*) the GZK effect (which limits trans-GZK observed sources to lie within a few 100 Mpc), (*b*) the anisotropic distribution of source-bearing galaxies on 100 Mpc scales, and (*c*) the low magnetic deflection of light trans-GZK nuclei by the Galactic and extragalactic magnetic fields. Therefore, the report of correlations between UHECRs above 55 EeV and the distribution of nearby active galaxies (Abraham et al. 2007) can be simply interpreted as protons from nearby sources within the so-called GZK sphere. However, composition indicators from shower development observations argue for a transition to a heavier component from around 4 EeV up to 40 EeV (Abraham et al. 2010a). Heavy nuclei-dominated injection models are quite rare in the

astrophysical literature of candidate sources (see Section 6), and if iron is the main component at the highest energies, Galactic magnetic fields should wash out most anisotropic patterns around 60 EeV. Another possible interpretation of the observed shower development properties is a change in hadronic interactions above 100 TeV center of mass (TeV $\equiv 10^{12}$ eV), an order of magnitude higher energy than will be reached by the Large Hadron Collider (LHC) at CERN. A new puzzle is born: An injection at the source dominated by heavy nuclei is astrophysically unexpected, while significant changes in hadronic interactions represent novel particle physics.

To help discriminate between possible interpretations of recent results, we review in Section 3 the well-known physics of the propagation of UHECRs: their interaction with the cosmic background radiation and the effect of cosmic magnetic fields. The effect of propagation on the observed spectrum, sky distribution, and composition depends on the source redshift evolution, the injected spectrum and composition, and the evolution of cosmic backgrounds and magnetic fields. The spectrum is cut off due to photo-pion production of protons and photodissociation of nuclei off cosmic backgrounds. The composition simplifies to either proton or iron (or a mixture of the two) at trans-GZK energies. Anisotropies in the sky distribution of sources are blurred by magnetic fields for heavier primaries, while protons keep most of the original anisotropies at trans-GZK energies.

Different scenarios for the transition between cosmic rays created in the Galaxy and those from extragalactic sources are discussed in Section 4. Specific acceleration mechanisms envisioned for reaching these extremely high energies are the topic of Section 5, including shock acceleration, unipolar inductors, and other proposals. In Section 6, we survey known astrophysical sites that are reasonable candidates for UHECR sources, from compact objects such as neutron stars (or magnetars), to gamma-ray bursts (GRBs) and active galaxies. Possible signatures of different candidate sources are discussed in light of future observations of UHECRs and other messengers of the extreme Universe.

With a significant increase in the integrated exposure to cosmic rays above 60 EeV, next generation observatories may reach the sensitivity necessary to achieve charged particle astronomy and to observe ultrahigh-energy photons and neutrinos, which may further illuminate the workings of the Universe at the most extreme energies. We end with the ongoing and future search plans for the cosmic sources of ultrahigh-energy particles.

Due to the limited space, we refer readers interested in details of observational techniques to Letessier-Selvon & Stanev (2011), Beatty & Westerhoff (2009), Bluemer, Engel & Hoerandel (2009), and Nagano & Watson (2000). Previous reviews on the astrophysics of UHECRs can be found in Cronin (2005), Olinto (2000), Berezinsky et al. (1990), and Hillas (1984, 2006), whereas Bhattacharjee & Sigl (2000) also include a survey of UHECRs from cosmological relics. Stanev (2010) published a recent monograph on UHECRs, and Gaisser (1991) covers cosmic rays of lower energies. Recent reviews cover the closely related high-energy neutrinos (Anchordoqui & Montaruli 2010) and high-energy gamma rays (Hinton & Hofmann 2009).

2. COSMIC RAY OBSERVATIONS AT ULTRAHIGH ENERGIES

After many decades of efforts to discover the origin of cosmic rays, current observatories are now reaching the necessary exposure to begin unveiling this longstanding mystery. The first detection of UHECRs dates back to Linsley (1963), but it was only during the 1990s that an international effort began to address these questions with the necessary large-scale observatories. The largest detectors operating during the 1990s were the Akeno Giant Air Shower Array (AGASA), a 100 km^2 ground array of scintillators in Japan (Chiba et al. 1992), and the High Resolution Fly's Eye (HiRes), a pair of fluorescence telescopes that operated in Utah until 2006 (Boyer et al. 2002).

During their lifetimes, AGASA reached an exposure of 1.6×10^3 km^2 sr year (or 1,600 L; in honor of UHECR pioneer John Linsley, we use the exposure unit $L = 1$ km^2 sr year), whereas HiRes reached twice that. To date, the highest energy recorded event was a 320 EeV fluorescence detection (Bird et al. 1994) by the pioneer fluorescence experiment Fly's Eye (Baltrusaitis et al. 1985).

Completed in 2008, the Pierre Auger Observatory (Auger) is the largest observatory at present (Abraham et al. 2004). Constructed in the province of Mendoza, Argentina, by a collaboration of 18 countries, it consists of a 3,000 km^2 array of water Cherenkov stations with 1.5 km spacing in a triangular grid overlooked by four fluorescence telescopes. The combination of the two techniques into a hybrid observatory maximizes the precision in the reconstruction of air showers, allowing for large statistics with good control of systematics. The largest observatory in the northern hemisphere, the Telescope Array (TA), is also hybrid (Nonaka et al. 2009, Tokuno et al. 2009). Situated in Utah, it covers 762 km^2 with scintillators spaced every 1.2 km overlooked by three fluorescence telescopes.

2.1. Spectrum

The observed cosmic ray spectrum (**Figure 1**) can be described by a broken power law, E^{-s}, with spectral index $s = 2.7$ below the knee at $\sim$1 PeV ($= 10^{15}$ eV) and $s \simeq 3$ between the knee and the ankle around 3 EeV (Apel et al. 2009). Above the ankle, $s \simeq 2.6$ followed by the recently established flux suppression above about 30 EeV. With exposures around 10^3 L, the measured spectra at energies where the GZK effect was anticipated had conflicting results: AGASA reported no flux supression at trans-GZK energies (Takeda et al. 1998), whereas early results from HiRes were consistent with the GZK prediction (Abbasi et al. 2004). By 2006, HiRes accumulated enough statistics for the first significant observation of the GZK suppression (Abbasi et al. 2008b), as displayed in **Figure 2**. This was confirmed by the Auger Observatory (Abraham et al. 2008a) with a recent update starting at 1 EeV (Abraham et al. 2010b) and based on 1.3×10^4 L exposure (shown in **Figure 2**). The displayed error bars are statistical errors, whereas the reported systematic error on the absolute energy scale is about 22%. This systematic error allows for overall energy shifts that make the two observations consistent within the estimated errors. The highest energy event reported by Auger thus far is of 142 EeV (Abreu et al. 2010).

Figure 2 also shows the observed spectrum fit by different models of UHECR sources (taken from Kotera, Allard & Olinto 2010 and references therein). In the mixed composition and iron-dominated models (Allard, Parizot & Olinto 2007), the ankle indicates a transition from Galactic to extragalactic cosmic rays (see Section 4), the source evolution is similar to the star-formation rate (SFR), and the injection spectra are relatively hard ($s \sim 2-2.1$). In the proton-dominated models in the figure, the ankle is due to pair production propagation losses (Berezinsky & Grigorieva 1988), named dip models (Berezinsky, Gazizov & Grigorieva 2006), and the injection spectra are softer for a wide range of evolution models. Models with proton primaries can also fit the spectrum with harder injection with a transition from Galactic to extragalactic at the ankle (Wibig & Wolfendale 2004).

The confirmed presence of a spectral feature similar to the predicted GZK cutoff settles the question of whether acceleration in extragalactic sources can explain the high-energy spectrum, ending the need for exotic alternatives designed to avoid the GZK feature. However, the possibility that the observed softening of the spectrum is mainly due to the maximum energy of acceleration at the source, $E_{\max}$, is not as easily dismissed. A confirmation that the observed softening is the GZK feature awaits supporting evidence from the spectral shape, anisotropies, and composition at trans-GZK energies and the observation of produced secondaries such as neutrinos and photons.

2.2. Anisotropies in the Sky Distribution

The landmark measurement of a flux suppression at the highest energies encourages the search for sources in the nearby extragalactic Universe using the arrival directions of trans-GZK cosmic rays. Above GZK energies, observable sources must lie within about 100 Mpc, the so-called GZK horizon or GZK sphere (Harari, Mollerach & Roulet 2006 and references therein). This effect is shown in **Figure 3**, where the fraction of cosmic rays that arrive on Earth from a given distance is plotted for different energy protons (>40, 60, and 100 EeV) and for different nuclei (He, CNO, and Fe) arriving with energies above 60 EeV. At these trans-GZK energies, light composite nuclei are promptly dissociated by cosmic background photons (see Section 3), whereas protons and iron nuclei may reach us from sources at distances up to about 100 Mpc. Because matter is known to be distributed inhomogeneously within this distance scale, the cosmic ray arrival directions should exhibit an anisotropic distribution above the GZK energy threshold, provided intervening magnetic fields are not too strong. At the highest energies, the isotropic diffuse flux from sources far beyond this GZK horizon should be strongly suppressed.

Attempts to detect anisotropies at ultrahigh energies date back to the mid-1990s, when hints of correlations with the local large-scale structure and with distant BL Lacs objects were claimed and debated (see Section 6.2). With the increase in the number of observed ultrahigh-energy events, these early claims have not been substantiated, and different correlations have been recently reported.

The most recent discussion of anisotropies in the sky distribution of ultrahigh-energy events began with the report that the arrival directions of the 27 cosmic rays observed by Auger with

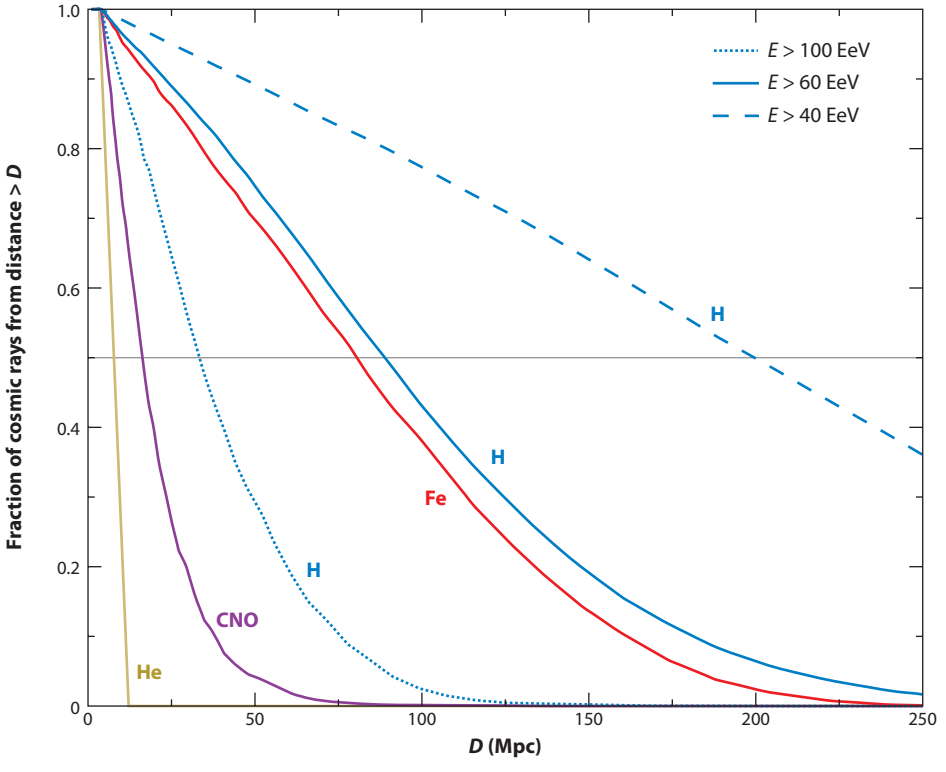

Figure 3

Fraction of cosmic rays that survives propagation over a distance $> D$, for protons above 40, 60, and 100 EeV and for He, CNO, and Fe above 60 EeV. The gray solid line shows where 50% of a given species can originate for a given atomic mass and energy. At trans-GZK energies ($E \gtrsim 60$ EeV), only protons and iron survive the propagation over $D \gtrsim 50$ Mpc.

energies above 57 EeV exhibited a statistically significant correlation with the anisotropically distributed galaxies in the twelfth VCV (Véron-Cetty & Véron 2006) catalog of active galactic nuclei (AGN) (Abraham et al. 2007, 2008c). The correlation was most significant for AGN with redshifts $z < 0.018$ (distances <75 Mpc) and within 3.1° separation angles. An independent dataset confirmed the anisotropy at a confidence level of over 99% (Abraham et al. 2007, 2008c). The prescription established by the Auger collaboration tested the departure from isotropy given the VCV AGN coverage of the sky, not the hypothesis that the VCV AGN were the actual UHECR sources. In particular, a lack of events from the Virgo region showed that assuming the VCV AGN to be the sources gives a bad match to the observed event distribution [D.S. Gorbunov, P.G. Tinyakov, I.I. Tkachev, S.V. Troitsky, unpublished (arXiv:0804.1088v1)]. No corresponding correlation was observed in the Northern Hemisphere by HiRes (Abbasi et al. 2008c), where the distribution of their 13 trans-GZK events is consistent with isotropy.

Figure 4 shows a map of the 69 events used in the recently published Auger update, which includes another 42 trans-GZK events (Abreu et al. 2010). With the new events, the correlation with the VCV catalog is not as strong for the same parameters as the original period (20 events correlate out of the original 27, whereas only 12 correlate out of the new 42). The data after the prescription period show a departure from isotropy at the 3-σ level. With the currently estimated correlation fraction of 38%, a 5-σ significance shall require at least another four years of Auger observations (Abreu et al. 2010).

The VCV catalog is not a catalog produced by an instrument or survey strategy, but an extensive compilation of known AGN in the literature. A better set of catalogs that give a more homogeneous and statistically complete survey of the nearby Universe over the large field of view of Auger has become recently available. In particular, the Swift-BAT catalog of AGN (Tueller et al. 2010) and the 2MASS Redshift Survey (2MRS) catalog of galaxies (Huchra et al. 2005) are two catalogs where correlations may become more meaningful (George et al. 2008, Abreu et al. 2010).

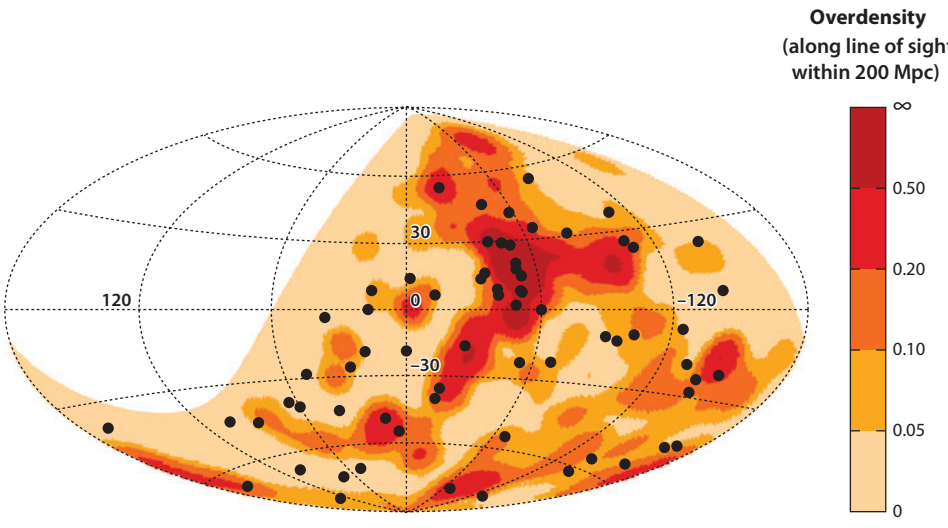

Figure 4

Arrival directions of cosmic rays with energy $E \geq 55$ EeV detected by the Pierre Auger Observatory (*black dots*) in an Aitoff-Hammer projection of the sky in Galactic coordinates restricted to $|b| > 10^{o}$. Shaded areas represent a smoothed density map of the 2MRS galaxies within 200 Mpc over the Auger Observatory field of view (Abreu et al. 2010). The angular smoothing scale is 5°.

Figure 4 shows the example of Auger data superimposed on a density map of AGNs within 200 Mpc from the 2MRS catalog (Abreu et al. 2010). These trans-GZK events tend to align better with the distribution of galaxies in 2MRS and with Swift-BAT AGN than with the isotropic scenario; however, the significance of the anisotropy or a source class identification is hard to access with the current limited statistics.

Finally, the anisotropy reported by the test with the VCV catalog may indicate the effect of the large-scale structure in the distribution of source harboring galaxies or it may be due to a nearby source. An interesting possibility is the cluster of Auger events around the direction of Centaurus A, the closest AGN (at ∼3.8 Mpc). The clustering around the Cen A region may also be due to the Centaurus cluster (as shown by the *dark red* region of **Figure 4**), which is much further away but in the general direction of Cen A (Kashti & Waxman 2008, Kotera & Lemoine 2008b). Only much higher statistics will tell if Cen A is the first UHECR source to be identified.

2.3. Composition

The third key measurement that can help resolve the mystery behind the origin of UHECRs is their composition as a function of energy observed on Earth. Composition measurements can be made directly up to energies of ∼100 TeV with space-based experiments (see, e.g., Ahn et al. 2010). For higher energies, composition is derived from the observed development and particle content of the extensive airshower created by the primary cosmic ray when it interacts with the atmosphere.

Presently, the best indicator of the composition of the primary particle is the depth in the atmosphere of the shower maximum, $X_{\rm max}$, given in grams per squared centimeter. The average shower maximum, $\langle X_{\rm max}\rangle$, scales approximately as ln (E/A), where E is the energy and A is the atomic mass of the primary cosmic ray that generated the shower (see, e.g., Letessier-Selvon & Stanev 2011 and references therein). On average, the shower maximum for protons occurs deeper in the atmosphere than that for the same energy iron nucleus, $\langle X^{p}_{\rm max}\rangle > \langle X^{Fe}_{\rm max}\rangle$. In addition, proton showers fluctuate more about $\langle X_{\rm max}\rangle$, providing another measure of composition, for example, the root mean square (rms) fluctuations about $\langle X_{\rm max}\rangle$. Another useful measure of composition is the particle content of the shower such as the number of muons: Proton showers have fewer muons than showers caused by heavier nuclei with the same energy. In practice, observed shower maxima and particle numbers are compared with Monte Carlo airshower simulations, which involve an extrapolation to higher energies of hadronic interactions known at energies of laboratory accelerators ($\lesssim$1 TeV).

Observations of shower properties from the knee to just below the ankle indicate a general trend from light primaries dominating at the knee to heavier primaries dominating up to ∼0.1 EeV (see, e.g., Bluemer, Engel & Hoerandel 2009). These observations follow expectations that the knee is created by a rigidity-dependent (rigidity is defined as particle momentum divided by charge, $\mathrm{R} \equiv p/Z \propto E/Z$) end of Galactic cosmic rays, which may be due to maximum acceleration at the sources and/or containment in the Galactic magnetic field. Just before the ankle, the trend seems to reverse back toward a lighter composition, being consistent with light primaries at 1 EeV as shown in **Figure 5**. **Figure 5** shows Auger data on $\langle X_{\rm max}\rangle$ and rms$(X_{\rm max})$ of 3,754 events above 1 EeV together with a range covered by simulations for protons and iron nuclei using different hadronic models (Abraham et al. 2010b). The dominance of light nuclei around 2 EeV is also observed by HiRes in their final reconstruction of 815 events by Abbasi et al. (2010).

A surprising trend occurs in Auger data above 10 EeV; a change toward heavy primaries is seen both in $\langle X_{\rm max}\rangle$ as well as in rms$(X_{\rm max})$ up to 40 EeV. As a mixture of different nuclei would

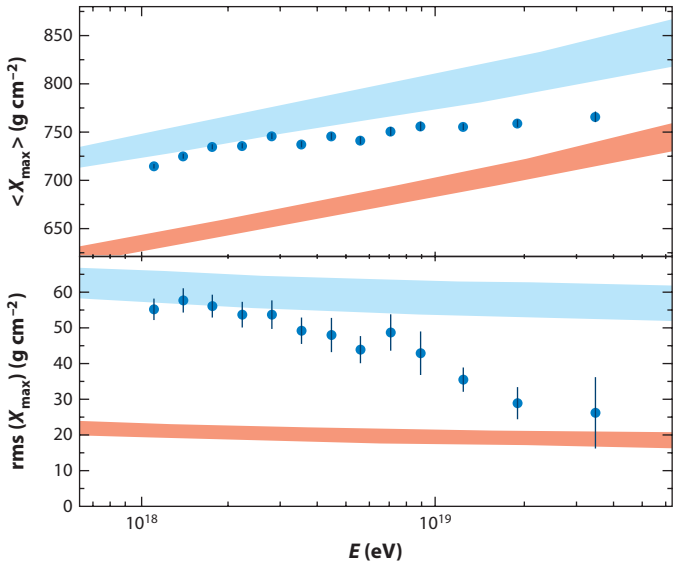

Figure 5

$\langle X_{max} \rangle$ and rms(X_{max}) as a function of primary energy, as measured by Auger Observatory fluorescence detectors (Abraham et al. 2010a). Monte Carlo simulations from different hadronic interaction models are displayed for primary protons (*light blue field*) and primary iron nuclei (*red field*).

increase the rms(X_{max}), the observed narrow distribution argues for a change toward a composition dominated by heavy nuclei. Due to different reconstruction methods, the HiRes measurement of fluctuations is not easily displayed in **Figure 5**, but the data trend remains closer to light primaries up to 60 EeV. The two results are consistent within quoted errors, so the situation is currently unclear.

Shower properties observed by Auger up to 40 EeV are quite challenging to candidate acceleration models because they conflict with the prevailing view that the primaries are proton dominated. The observed hint of anisotropies also points to light primaries (Abreu et al. 2010). Studies of ultrahigh-energy nuclei propagation require unusual choices in attempts to fit the observed composition indicators, such as a hard injection spectrum ($s \sim 1.6$) with primaries dominated by nitrogen or silicon (Hooper & Taylor 2010). Given the measurement uncertainties, some reasonable but disappointing options are also possible such as models where protons have a low maximum energy and the observed steepening of the spectrum, above 30 EeV, is due to the maximum energy of iron nuclei [Allard et al. 2008; also Aloisio, Berezinsky & Gazizov (2011) and D. Allard, unpublished (arXiv 0906.3156)]. In this case, the feature in the observed spectrum is mainly due to the maximum accelerator energy, which is coincidently close to the expected GZK cutoff. As discussed in Section 6, most known astrophysical accelerators have E_{max} close to GZK energies, so the coincidence may actually be real. The challenge to extragalactic candidate sources is to explain the origin of such high metallicities in the accelerated material. These observations have also motivated a return to the possibility that Galactic cosmic ray sources significantly contribute at ultrahigh energies (Calvez, Kusenko & Nagataki 2010).

As recently highlighted by Schwarzschild (2010), changes to hadronic interactions from current extrapolations provide a plausible alternative interpretation to the observed shower development behavior. Auger probes interactions above 100 TeV center of mass, whereas hadronic interactions are only known around 1 TeV. The observation of anisotropies and secondary particles (neutrinos and gamma rays) can lead to astrophysical constraints on the composition of UHECRs, opening the possibility for the study of hadronic interaction cross sections, multiplicities, and other interaction parameters at hundreds of teraelectronvolts.

The detailed composition of UHECRs is still to be understood, but it is clear that primaries are not dominated by photons (Abraham et al. 2008, 2009c) or neutrinos (Abraham et al. 2009b, Abbasi et al. 2008a). Limits on the photon fraction place stringent limits on models where UHECRs are generated by the decay of super heavy dark matter and topological defects. Unfortunately, the uncertainties on the UHECR source composition, spectrum, and redshift evolution translate to many orders of magnitude of uncertainty in the expected cosmogenic neutrino flux as discussed in Section 6.

3. THE PROPAGATION OF ULTRAHIGH-ENERGY COSMIC RAYS

While propagating from their sources to the observer, UHECRs experience two types of processes: (*a*) interactions with cosmic backgrounds that affect their energy and their composition, but not their direction, and (*b*) interactions with cosmic magnetic fields that affect their direction and travel time, but not their energy and composition. Both leave a variety of signatures on the observables of UHECRs and generate secondary neutrinos and gamma rays (see Section 6.3).

3.1. Interaction Processes on Cosmic Backgrounds

In the intergalactic medium (IGM), cosmic rays primarily interact with the Cosmic Microwave Background (CMB) photons at the highest energies, and with IR, optical, and UV background (IR-UV) photons at slightly lower energy (see, e.g., Kneiske et al. 2004 and Stecker, Malkan & Scully 2006 for detailed background models).

Photohadronic interactions between protons and background photons mainly lead to pion production ($p\gamma \rightarrow N + n\pi$; here N is a nucleon and n is the number of pions produced) or to electron-positron pair production (also called Bethe-Heitler process; $p\gamma \rightarrow pe^+e^-$). The energy threshold of these interactions for a photon of energy ϵ reads $E_{p,\pi} \sim 200\,\mathrm{EeV}\,(\epsilon_{\rm CMB}/\epsilon)$ for pion production, and for pair production $E_{p,\mathrm{ee}} \sim 0.8\,\mathrm{EeV}\,(\epsilon_{\rm CMB}/\epsilon)$, with $\epsilon_{\rm CMB} \simeq 2.7\,k_B T_{\rm CMB} \sim 6 \times 10^{-4}$ eV, the mean energy of a CMB photon.

We plot in **Figure 6** the energy loss lengths $x_{\rm loss} \equiv |E^{-1}\mathrm{d}E/c\,\mathrm{d}t|^{-1}$ for these two processes, using analytical formulae by Stecker (1968) (also see Maximon 1968; Genzel, Joos & Pfiel 1973; Begelman, Rudak & Sikora 1990; Mücke et al. 1999). Above $E \sim 60$ EeV, the distance that particles can travel without losing their energy shortens considerably. If cosmic rays originate from cosmological distances, their flux above this energy should be consequently suppressed, producing the well-known GZK feature in the UHECR spectrum (see Section 2.1). This property further imposes that the sources of the observed UHECRs at a given energy should be located in our local Universe, within a distance $l \lesssim x_{\rm loss}(E)$. Losses due to the cosmological expansion are also represented in **Figure 6**.

For primary cosmic rays with mass number $A > 1$, different interaction processes come into play. At ultrahigh energies, nuclei photo-disintegrate on CMB and IR-UV photons through three main types of processes that contribute at increasing energy ranges: the Giant Dipolar Resonance (for $\epsilon \sim 8-30$ MeV), the Quasi Deuteron process (for $\epsilon \sim 20-150$ MeV), and the Baryonic Resonance (for $\epsilon \sim 150$ MeV). In a first approximation, one can consider that the Lorentz factor of the primary nucleus remains unchanged through these interactions. Nuclei also experience photo-pair production that decreases the Lorentz factor without affecting the number of nucleons.

After pioneering work by Puget, Stecker & Bredekamp (1976), energy losses for nuclei have been examined by several groups [Stecker & Salamon 1999; Epele & Roulet 1998a,b; Bertone et al.

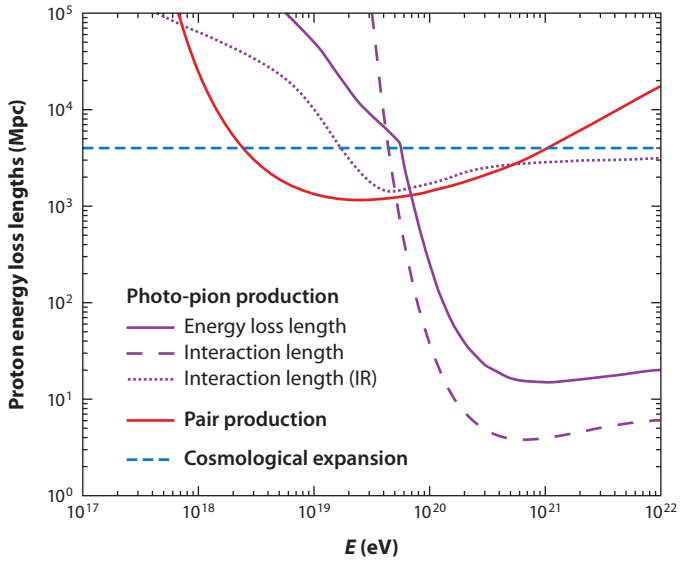

Figure 6

Proton energy loss lengths: purple lines show energy loss (*solid line*) and interaction lengths for photo-pion production on microwave background (*dashed line*) and IR-UV photons (*dotted line*); red solid line for pair production on CMB photons, assuming the background of Stecker, Malkan & Scully (2006). The dashed blue line indicates the losses due to cosmological expansion.

2002; Khan et al. 2005; Allard et al. 2005, 2008; Hooper, Taylor & Sarkar 2005; Hooper, Sarkar & Taylor 2008; see also R. Aloisio, V. Berezinsky, A. Gazizov, unpublished (arXiv 0803.2494)]. One remarkable effect of the propagation of nuclei is that nuclei with mass number $A < 20$ cannot travel farther than a few tens of megaparsecs without disintegrating (see **Figure 3**). In particular, one can conclude that heavy nuclei could be found in abundance at trans-GZK energies only if the composition were essentially dominated by iron group nuclei. Such a composition can arise when the proton $E_{\max}$ is smaller than $E_{p,\pi}$, so that only heavy nuclei are present at greater energies (Allard et al. 2008; Aloisio, Berezinsky, & Gazizov 2011).

The effect of photo-hadronic interactions on the cosmic ray spectrum can be calculated analytically for protons (Berezinsky & Grigorieva 1988; Berezinsky, Gazizov & Grigorieva 2006). Numerical codes such as SOPHIA (Mücke et al. 1999) enable the precise evaluation of the cross sections for photo-hadronic interactions, taking into account various channels, and of the produced flux of secondary particles (pioneered by Berezinsky & Gazizov 1993). Numerical Monte-Carlo methods are best suited to model inhomogeneous distribution of sources, calculate secondary emissions, and treat the complex processes intervening in the propagation of nuclei in the IGM. Among the existing propagation codes that have been developed for this purpose, one might refer to the public code CRPropa (Armengaud et al. 2007).

The calculated spectra are in very good agreement with the observed spectra for a variety of chemical compositions, Galactic to extragalactic transition models, source evolution histories, and injection spectrum indices between 1.6–2.7, for a fixed maximum acceleration energy, $E_{\max}$ (see, e.g., **Figure 2**). Kachelrieß & Semikoz (2006) demonstrate that relaxing the assumption of a single maximum acceleration energy and introducing a power-law distribution of $E_{\max}$ lead to a change

in the overall propagated spectrum slope. A key region for models to fit is the ankle around 4 EeV, where the spectral slope changes (see Section 4). The precise shape of the GZK feature depends on the local source density and on the transient or continuously emitting natures of the sources [see, e.g., Berezinsky, Gazizov & Grigorieva 2006; Blasi, Burles & Olinto 1999; Medina-Tanco 1998; Miralda-Escudé & Waxman 1996; also R. Aloisio, D. Boncioli, unpublished (arXiv 1002.4134)]. For instance, if $E_{\max} \gg 100$ EeV, a recovery of the spectrum at high energies can be observed by future detectors.

3.2. The Effects of Magnetic Fields

The absence of powerful astrophysical counterparts in the arrival directions of UHECRs is probably related to the effect of cosmic magnetic fields that deflect and delay particles during their propagation. Charged particles are subject to the influence of magnetic fields in the source environment, in the IGM, and in the Galaxy. Because very little is known about cosmic magnetic fields (for recent reviews see, e.g., Kronberg 1994; Widrow 2002; Vallée 2004; Kulsrud & Zweibel 2008; Beck 2008), the parameter space for an accurate description is quite large. Different propagation regimes apply to different cosmic ray rigidities, from weak angular deflection at the highest energies or in weak magnetic fields, to the diffusive regime in strong fields or at low enough energies.

Much progress has been made in recent years on Galactic magnetic field observations (see Han, Manchester & Qiao 1999; Han et al. 2006; Han 2008; Jansson et al. 2009) and their effect on the propagation of UHECRs (Harari, Mollerach & Roulet 1999; Alvarez-Muñiz, Engel & Stanev 2002; Tinyakov & Tkachev 2002, 2005). These studies conclude that the deflection for particles of charge Z and energy E should not exceed $\sim 10^\circ\, Z\,(40\,\mathrm{EeV}\,E^{-1})$. In particular, the regular component of the Galactic magnetic field can distort the angular images of cosmic ray sources: The flux may appear dispersed around the source or globally translated in the sky with a small dispersion (Harari, Mollerach & Roulet 1999). Galactic magnetic fields are not uniform in the sky, which implies that angular deflections depend on the observed direction (Harari, Mollerach & Roulet 1999; Kachelrieß, Serpico & Teshima 2007; Takami & Sato 2008).

The extragalactic magnetic field [EGMF, also called the intergalactic magnetic field (IGMF)] is less well known. Measurements of Faraday rotation provide estimates of the magnetic fields in the core of clusters of galaxies, with typical strengths $\sim$1–40 μG (see above reviews). Outside clusters, upper limits on the integrated strength of the magnetic field parallel to the line of sight, $B_{||}$, have been obtained using rotation measures (Ryu, Kang & Biermann 1998; Blasi, Burles & Olinto 1999): $\langle B_{||}^2 \lambda_B \rangle^{1/2} \lesssim 10^{-8}\,\mathrm{G\,Mpc}^{1/2}$, where the field reversal scale is $\lambda_B \lesssim 1$ Mpc, given the typical turbulent velocities (e.g., Waxman & Bahcall 1999). The future Square Kilometer Array project (Beck, Gaensler & Feretti 2007) will enlarge considerably the observations of the EGMF in our local Universe. Meanwhile, Neronov & Semikoz (2009) demonstrated that the observation of extended gamma-ray emission around point sources together with time delays in gamma-ray flares should provide robust measurements of the EGMF and help constrain scenarios of its origin. These new developments may lead to stronger constraints or even detections of the EGMF, which at present can range from 10^{-16}–10^{-9} G.

The origins of extragalactic magnetic fields are not well understood (e.g., Kulsrud & Zweibel 2007). Some models set their origins in the primordial Universe (see Widrow 2002 and references therein); other models through magnetic pollution from astrophysical sources such as galactic winds or jets from radio galaxies (Kronberg, Lesch & Hopp 1999; Birk et al. 2000; Aguirre et al. 2001; Bertone, Stoehr & White 2005; Cen, Nagamine & Ostriker 2005; Bertone, Vogt & Enßlin 2006; Scannapieco et al. 2006). If magnetic fields have a primordial origin, they should be

all-pervading and amplified in dense regions by dynamical effects induced by large-scale structure formation. If galaxies are the primary generators of magnetic enrichment, the field should be rather concentrated in high-peaked density regions and nearly suppressed in voids, depending on the efficiency of the winds (Bertone, Vogt & Enßlin 2006). A combination of the two scenarios may occur, as well as intermediate models in which magnetic pollution happens during the reionization epoch, generating slightly inhomogeneous fields already at high redshift. Whatever the origin of extragalactic fields, dynamical amplification in dense regions during structure collapse should play a key role in setting up their present configuration (Bruni, Maartens & Tsagas 2003; Siemieniec-Oziebło & Golda 2004; King & Coles 2006; Ryu et al. 2008).

The structure and strength of the EGMF can strongly affect the propagation of UHECRs. Early simulations of cosmic ray propagation in EGMFs considered homogeneous magnetic fields or the lensing effect of the magnetized local supercluster (Lemoine et al. 1997; Medina-Tanco et al. 1997; Sigl, Lemoine & Olinto 1997; Medina-Tanco 1998; Sigl, Lemoine & Biermann 1999; Ide et al. 2001; Isola, Lemoine & Sigl 2002; Isola & Sigl 2002; Stanev, Seckel & Engel 2003). Analytical works by Wdowczyk & Wolfendale (1979), Blasi & Olinto (1999), Waxman & Miralda-Escudé (1996), Harari, Mollerach & Roulet (2002), Harari et al. (2002), Kotera & Lemoine (2008b), and Aharonian, Kelner & Prosekin (2010) have helped to establish the influence of the EGMF on observable UHECR quantities.

More recently, various groups have developed simulations of the formation of large-scale structures, including magnetic fields, in order to model more realistic inhomogeneous configurations (Ryu, Kang & Biermann 1998; Sigl, Miniati & Enßlin 2004; Dolag et al. 2004, 2005; Brüggen et al. 2005; Dubois & Teyssier 2008; Das et al. 2008; Ryu et al. 2008; Donnert et al. 2009). Most of these researchers set an initial magnetic seed at high redshift that is then evolved in time. The overall amplitude of the field is rescaled at the end of the simulation so as to reproduce the observed strength of magnetic fields in the core of clusters of galaxies. Ryu, Kang & Biermann (1998) and Das et al. (2008) estimate directly the intensity of the magnetic field using the vorticity and the energy density calculated from the kinetic properties of the gas. With these methods, magnetic fields generated by astrophysical feedback can be hard to implement (see, however, Donnert et al. 2009, who have incorporated some of these effects).

These simulations lead to very discrepant results concerning the configuration of the fields (see **Figure 7**). These differences probably stem from the different methods and assumptions made by each group, and illustrate the inherent complexity of these simulations. Indeed, Ryu, Kang & Biermann (1998) and Sigl, Miniati & Enßlin (2004) assume that magnetic seeds are generated by Biermann battery effects around accretion shocks, whereas Dolag et al. (2005) implement a homogeneous seed around redshift $z \sim 20$, and Donnert et al. (2009) add to the latter method astrophysical magnetic pollution in localized spots at lower redshifts. The difference in configuration probably also results from the Eulerian and Lagrangian treatments used by the different groups and limitations on dynamical range and resolution.

Such discrepancies on the magnetic fields impact the range of deflections induced on UHECRs. For instance, Sigl, Miniati & Enßlin (2004) find that protons with energy $E > 100$ EeV should be deflected by 10–20°, whereas Dolag et al. (2004) find deflections of less than a degree at the same energy.

In the framework of UHECR propagation, a simpler and faster approach to model the inhomogeneous extragalactic magnetic field entails performing a scaling of the field strength to the underlying density field (Takami, Yoshiguchi & Sato 2006; Takami & Sato 2008; Kotera & Lemoine 2008a; also G.A. Medina-Tanco, 1997, arXiv:9707054). The assumed scaling law enables one to account for various types of magnetic field amplifications due to structure collapse and for the high contrast fields that should be produced by astrophysical pollution. In addition, an analytic

Figure 7

Cumulative volume filling factor of the extragalactic magnetic field for different numerical simulations.

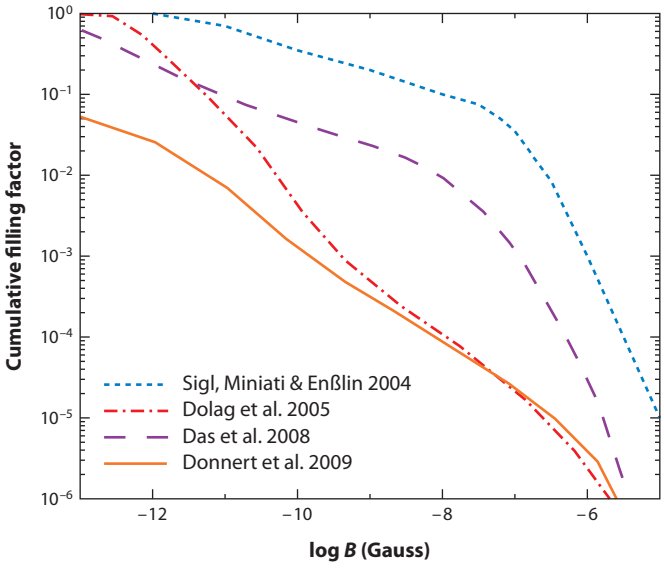

stochastic approach can be effective in describing the propagation of UHECRs in the extragalactic fields because of the high energy of the particles and the low magnetization of voids (Kotera & Lemoine 2008b). Indeed, the deflection of UHECRs by magnetic fields of strength $B < 10^{-12}$ G is lower than typical instrument resolutions, which are ∼1°. Particle transport can then be viewed as a succession of rectilinear portions interrupted by deflections on localized magnetized regions (such as filaments, halos of radio galaxies and galactic winds). This model can be applied to the coherent field amplified in numerical simulations as well as to the local enrichment processes due to astrophysical sources, and provides an effective framework to calculate the influence of magnetic fields on observable quantities of UHECRs.

4. THE GALACTIC TO EXTRAGALACTIC TRANSITION

The highest energy cosmic rays are likely to originate in extragalactic sources, given the strength of Galactic magnetic fields and the lack of correlations with the Galactic plane. Low-energy cosmic rays are easily created and contained in the Galaxy, so a transition region should occur in some intermediate energy. "A hypothesis blessed by long tradition is that" Galactic cosmic rays end below 10 EeV, "and above that a different source is active (most plausibly in the nearby supercluster of galaxies)," quoting Hillas (1984). Modern measurements of the spectrum place a plausible transition region around the ankle at about 4 EeV (**Figures 1** and **2**). However, the ankle can also be interpreted as the product of propagation losses due to pair production (Berezinsky & Grigorieva 1988; Berezinsky, Gazizov & Grigorieva 2006) in proton-dominated scenarios allowing for a transition at lower energies.

The knee in the cosmic ray spectrum is likely to signal the $E_{\rm max}$ for light nuclei of dominant Galactic sources and/or the maximum containment energy for light nuclei in the Galactic magnetic field. The same effect for heavier nuclei may cause the softer spectrum above the knee (see, e.g., Lemoine 2005, Hillas 2006). Extragalactic sources producing spectra harder than $s = 3$ can overtake the decaying Galactic flux around the ankle. Recent studies of a transition at the ankle that fit the observed spectrum and the composition trends in this energy region are discussed by

Allard et al. (2005), where different models are contrasted. Models based on proton primaries with a hard spectrum (Wibig & Wolfendale 2004), on a mixed composition with proportions similar to the Galactic mix, or even on a composition dominated by heavy nuclei (Allard, Parizot & Olinto 2007) fit well with the UHECR spectrum and composition data around the ankle. In **Figure 2**, we show two examples of the so-called ankle transition models: one with source injection $s = 2.1$ (a source composition similar to the Galactic mixture) and source evolution that follows the star-formation rate; and a second model with similar source evolution and $s = 2$, but a pure iron composition injected. Both models fit well the UHECR spectrum but predict different compositions throughout this energy range.

Ankle transition models work well for UHECR scenarios, but they were thought to challenge models for the origin of Galactic cosmic rays. The requirement that Galactic sources reach energies close to the ankle strained traditional models, where acceleration in supernova remnants (SNRs) was expected to fade around 1 PeV (Lagage & Cesarsky 1983). A modification to the traditional SNR scenario, such as magnetic field amplification in SN shocks (Bell & Lucek 2001) or a different progenitor such as Wolf-Rayet star winds (Biermann & Cassinelli 1993), and trans-relativistic supernovae (Budnik et al. 2008) may explain the energy gap from PeV to EeV. Taking into account magnetic field amplification and Alfvénic drift in shocks of Type IIb SNRs, Ptuskin et al. (2010) find that Galactic cosmic ray iron can reach $E_{\max} \sim 5$ EeV, allowing extragalactic cosmic rays to begin to dominate above the ankle.

The possibility that the ankle is due to pair-production losses during the propagation of extragalactic protons (Berezinsky & Grigorieva 1988) has motivated an alternative model for the Galactic to extragalactic transition, called dip models (Berezinsky, Gazizov & Grigorieva 2006). The energy of the predicted dip is close to the observed ankle, and a good fit to the spectrum over a large energy range is reached with a softer injection index as shown in the dip proton models in **Figure 2**. This option relaxes the need for Galactic cosmic rays to reach close to EeV energies; however, it needs to be tuned to avoid strong (unobserved) spectral features between the knee and the ankle. Detailed models where the lower energy behavior of the extragalactic component blends smoothly with the Galactic cosmic rays have been developed using minimum energy and magnetic effects (Lemoine 2005; Aloisio & Berezinsky 2005; Hillas 2006; Kotera & Lemoine 2008a; Globus, Allard & Parizot 2008). In some of these models, a feature is produced around the second knee, which may be observed around 0.5 EeV. The dip model can fit the observed spectrum if the injection is proton dominated (Berezinsky, Gazizov & Grigorieva 2005; Allard, Parizot & Olinto 2007) or with at most a primordial proton to helium mix (Hillas 2006), which gives a clear path for distinguishing it from mixed composition models. A proton-dominated flux below the ankle region is a necessary condition for this model to be verified.

Clarifying the structure of the transition region is crucial for reaching a coherent picture of the origin of Galactic and extragalactic cosmic rays. This requires accurate spectrum and composition measurements from the knee to the ankle and beyond. KASCADE-Grande (Apel et al. 2009) has made great progress above the knee, but UHECR projects have started to lower their energy threshold as is being done with the Auger Observatory enhancements (Abraham et al. 2009a): HEAT (High Elevation Auger Telescopes) and AMIGA (Auger Muons and Inll for the Ground Array), and the Telescope Array Low Energy Extension (TALE) proposal. Having the same system covering a large range in energy helps control systematic offsets that degrade the accuracy of the needed precision. In addition, a strong multiwavelength program has shown that magnetic field amplification occurs in SNRs, and Galactic sources can reach further than previously believed. Finally, models of hadronic interactions will benefit by the energy reach of the LHC, which can probe hadronic interactions at energies higher than the knee (**Figure 1**) and help constrain composition indicators between the knee and the ankle.

5. ACCELERATION MECHANISMS

The acceleration of charged particles is easily achieved in the presence of electric fields. However, ubiquitous astrophysical plasmas destroy large-scale electric fields throughout the Universe. Occasionally, high voltage drops that may lead to particle acceleration can be found in some regions of the magnetosphere or the wind of neutron stars, or near black holes and their accretion disks. In contrast, magnetic fields are omnipresent in astrophysical objects. Their variations in space and time imply the existence of transient electric fields that can supply a consequent amount of energy to charged particles.

In our framework, acceleration mechanisms must fulfill the following criteria: They should enable charged particles to reach ultrahigh energies (from 1 to above 200 EeV), and the accelerated population should bear an injection spectrum (usually power law) that would fit the observed UHECR spectrum after propagation. Below we summarize two of the most commonly cited acceleration mechanisms, Fermi acceleration (see Section 5.1) and unipolar inductors (see Section 5.2), and briefly discuss other processes that have been proposed in the literature (see Section 5.3).

5.1. Fermi Acceleration at Shock Waves

The principle of Fermi acceleration is the transfer of energy from macroscopic motion to microscopic particles through their interaction with magnetic inhomogeneities. In the version elaborated by Fermi himself (Fermi 1949), magnetic scattering centers had random velocities that led to an energy gain of order $\Delta E/E \propto \beta^2$, where β is the average velocity of the scattering centers in units of c. This process is now called second-order Fermi acceleration, whereas the first-order Fermi process is the case where the macroscopic motion is coherent, such as a shock wave where particles can gain energy as they bounce back and forth, making $\Delta E/E \propto \beta$ (Axford, Leer & Skadron 1977; Bell 1978; Blandford & Ostriker 1978). Shock waves are quite frequent in the Universe, for instance, where an ejecta encounters the interstellar medium. SNR shocks are believed to be the sites where Galactic cosmic rays are accelerated via first-order Fermi processes. Popular shock regions for UHECR acceleration are GRB shocks, jets and hot spots of AGN, and gravitational accretion shocks.

Second-order Fermi acceleration depends on the scattering time of particles in the magnetic turbulence and, thus, on the characteristics of the latter, which are poorly known in astrophysical objects. It is less efficient than first-order Fermi in the nonrelativistic limit ($\beta \ll 1$). In the relativistic case (Pelletier 1999), it has been applied to acceleration studies inside GRBs (Pelletier & Kersalé 2000; Gialis & Pelletier 2003, 2004, 2005).

First-order Fermi processes under the test particle approximation (i.e., assuming that the density of accelerated particles is negligible compared to the thermal energy of the plasma in which the shock propagates, and hence that they do not produce a back-reaction on the shock) lead to simple power-law predictions for the spectrum of the accelerated population (see, e.g., Gaisser 1991). Several recent studies show that first-order Fermi acceleration at relativistic shock waves is more intricate, even under the test particle approximation (Gallant & Achterberg 1999; Lemoine & Pelletier 2003; Lemoine, Pelletier & Revenu 2006; Pelletier, Lemoine & Marcowith 2009). Lemoine, Pelletier & Revenu (2006) have pointed out that Fermi acceleration cannot happen if the Larmor radius of the accelerated particle is much smaller than the coherence length of the magnetic field. Indeed, the particle is then captured on a field line and advected far away downstream because the magnetic field is shock-compressed to a perpendicular configuration. Fermi acceleration should thus stop after a first back and forth cycle around the shock, unless

the magnetic field is strongly amplified on spatial scales much smaller than the Larmor radius r_L of the particle. It was further demonstrated by Pelletier, Lemoine & Marcowith (2009) that the noise associated with the motion in the small-scale turbulent magnetic field needs to overcome the unperturbed trajectory in the large-scale coherent field, which sets an upper bound to r_L (see also Niemiec, Ostrowski & Pohl 2006).

Such requirements being hardly reached for ultrarelativistic shocks, as discussed by Pelletier, Lemoine & Marcowith (2009), one might advocate that the most efficient Fermi acceleration occurs around mildly relativistic shocks. The characteristics of the accelerated population strongly depend on shock parameters (e.g., the shock Lorentz factor Γ_{sh}, temperature, and pressure values). No general tendency is easily derived, as can be concluded from the large span of spectral properties obtained by the groups who have performed detailed studies of particle acceleration around mildly relativistic shocks in various situations (e.g., Bednarz & Ostrowski 1998, Kirk et al. 2000).

Accelerated particles can act as precursors of the shock and induce significant modifications of the gas flow upstream and downstream. The current of energetic particles can initiate plasma instabilities that tend to increase the level of magnetohydrodynamic (MHD) turbulence, which scatter the particles. The possibility that streaming instabilities amplify the magnetic field, and that the acceleration efficiency could increase accordingly, was first discussed in the framework of nonrelativistic shocks in SNRs (Bell 1978, Lagage & Cesarsky 1983). More detailed work was conducted by, e.g., McKenzie & Völk (1982), Berezhko & Ellison (1999), Lucek & Bell (2000), Malkov & O'C Drury (2001), Bell & Lucek (2001), Bell (2004), Amato & Blasi (2005, 2006, 2009), Zirakashvili, Ptuskin & Völk (2008), and Reville et al. (2008). The estimated amplification of the upstream field is at most of two orders of magnitude. The generalization of the instability to the relativistic regime (Milosavljević & Nakar 2006; Reville et al. 2007; Pelletier, Lemoine & Marcowith 2009) reveals that this mechanism is not sufficient to allow efficient first-order Fermi acceleration around ultrarelativistic shocks. Other mechanisms outside the MHD range, such as Weibel-like instabilities (Medvedev & Zakutnyaya 2009) or resonant Cerenkov effects with plasma modes (Pelletier, Lemoine & Marcowith 2009) might yet provide enough amplification to allow successful Fermi acceleration. The relativistic two stream Weibel instability could amplify the magnetic field on small scales, to the level required by afterglow modeling of GRBs (Gruzinov & Waxman 1999, Medvedev & Loeb 1999). In order to make progress on these issues, many groups are performing Particle-In-Cell simulations that endeavor to solve self-consistently the field-particle interactions (e.g., Silva et al. 2003; Hededal & Nishikawa 2005; Dieckmann, Shukla & Drury 2008; Spitkovsky 2008; Riquelme & Spitkovsky 2010). It is promising that the latest simulations see evidence of Fermi acceleration and particle-wave interactions.

Finally, when modeling Fermi acceleration around shocks, mechanisms of shear acceleration have to be taken into account. Particles traversing a velocity gradient perpendicularly to a jet axis (instead of going along the axis as in the case of pure shock acceleration) can experience acceleration (e.g., Rieger, Bosch-Ramon & Duffy 2007; see Rieger & Duffy 2005 for an application to acceleration of UHECRs in GRBs and Lyutikov & Ouyed 2007 for a variant). This mechanism, however, depends on the characteristics of the plasma velocity gradients, which are not fixed, unlike the shock characteristics.

5.2. Unipolar Inductors

Unipolar inductors have been suggested as alternative ways to accelerate particles to ultrahigh energies (see, e.g., Berezinsky et al. 1990). Here we focus specifically on neutron stars, but acceleration may also be caused by unipolar inductors in other relativistic magnetic rotators, such as black holes with magnetized disks that lose rotational energy in jets.

Rapidly rotating neutron stars generally create relativistic outflows (winds), where the combination of the rotational energy and the strong magnetic field induces an electric field $\mathbf{E} = -\mathbf{v}\times\mathbf{B}/c$ (where $\mathbf{v}$ and $\mathbf{B}$ are the velocity and the magnetic field, respectively, of the outflowing plasma). The wind thus presents voltage drops where charged particles can be accelerated to high energy. This model was first developed in the framework of ordinary pulsars (see, e.g., Shapiro & Teukolsky 1983 and references therein), but the latter do not supply enough energy to reach the highest energies ($E > 10^{20}$ eV). Blasi, Epstein & Olinto (2000) pointed out that young neutron stars with millisecond rotation periods Ω and very high-surface magnetic fields B_* (i.e., magnetars) could easily accelerate particles to: $E(\Omega) \sim 3\times10^{21}\ \mathrm{eV}\ Z\eta_1(B_*/2\times10^{15}\ \mathrm{G})(R_*/10\,\mathrm{km})^3(\Omega/10^4\,\mathrm{s}^{-1})^2$, where $\eta_1 = 0.1$ is the fraction of the voltage drop experienced by a particle and R_* is the radius of the star. The spin down of the magnetar due to energy losses and the dependency of the particle acceleration energy on Ω lead to a power-law spectrum for the population of cosmic rays produced by a magnetar (Blasi, Epstein & Olinto 2000; Arons 2003): $dN/dE = 9c^2 I(1+E/E_\mathrm{g})^{-1}(2\,Ze\,B_*R_*^3E)^{-1}$. I is the principal inertial momentum of the magnetar and E_g is the energy corresponding to its angular velocity, at which gravity wave losses and electromagnetic losses are equal. Arons (2003) calculated that UHECRs should be produced at the very early stages of the lives of magnetars (after a few days to get down to $E \sim 6$ EeV); hence their emission can be considered as an impulsive burst. Note that this model was introduced in the AGASA era, in order to explain the absence of the GZK cutoff; with our current data however, such a hard injection spectrum ($s = 1$) is problematic as it does not fit the observed slope. An adequate distribution of initial voltages among magnetars can be found to soften the spectrum, that could still lead to detectable gravitational waves (Kotera, 2011, arXiv:1106.3060).

The toy model described above needs to be further investigated on several issues, for instance, on the nature of the ions injected in the wind, on the mechanism through which the current in the wind taps the available voltage, and on the escape of the accelerated particles from the wind and the wind nebula. Such issues are discussed in detail by Arons (2003).

5.3. Other Models

Among other models that have been proposed in the literature, one might consider magnetic reconnection acceleration, wake-field acceleration (often related to ponderomotive acceleration), and reacceleration in sheared jets. In a plasma, a local reconfiguration of the magnetic field topology (or reconnection) happens when the plasma conductivity is not high enough to support the current associated with a magnetic field structure (see Zweibel & Yamada 2009 for a review). The field reaches a lower energy-level configuration, and the liberated energy can be devoted to particle acceleration. This mechanism, responsible for the generation of high-energy particles in solar flares, has been applied to UHECR acceleration in pulsar winds (Coroniti 1990, Lyubarsky & Kirk 2001), in newborn millisecond pulsars (de Gouveia Dal Pino & Lazarian 2000), in termination shocks of pulsar winds (Lyubarsky 2003), and in GRB outflows (Thompson 2006). Some researchers also proposed that, in Poynting-flux-dominated flows (e.g., flows with Poynting to kinetic flux ratio $\gtrsim$1), first-order Fermi acceleration could aliment this mechanism, as particles reflected in the magnetized plasma could converge in the reconnection region (de Gouveia Dal Pino & Lazarian 2005, Giannios 2010).

A wake-field is created in a plasma when waves with high charge separation travel through the plasma. It leads to the formation of ponderomotive forces (longitudinal Lorentz invariant nonlinear forces that a charged particle experiences in an inhomogeneous oscillating electromagnetic field) that can accelerate particles if they are trapped in the wave: particles surf-ride the waves (Tajima & Dawson 1979; Chen, Tajima & Takahashi 2002). A simple form of surf-riding acceleration was

developed in the case of a pulsar wind by Buckley (1977) and by Contopoulos & Kazanas (2002). A detailed discussion of magnetar winds is also made by Arons (2003).

Other acceleration mechanisms have been proposed and may contribute to the acceleration of cosmic rays in the Galaxy. These include a variety of second-order processes and many of them can be observed to operate in solar physics. However, they are believed to be too slow to be relevant to the acceleration of UHECRs.

6. CANDIDATE SOURCES AND THEIR SIGNATURES

The requirements for astrophysical objects to be sources of UHECRs are quite stringent. After reviewing some of the basic requirements in Section 6.1, we briefly discuss plausible sources such as accretion shocks in large-scale structures (Section 6.1.1), AGN (Section 6.1.2), GRBs (Section 6.1.3), and neutron stars or magnetars (in Section 6.1.4). For these different classes of candidate sources, we discuss the possibility of locating the sources with UHECR observations in Section 6.2 and review possible ways of discovering the sources with secondary photons and neutrinos in Section 6.3.

6.1. Candidate Source Requirements

The Larmor radius, $r_L = E/ZeB \sim 110\ \mathrm{kpc}\ Z^{-1}(\mu\mathrm{G}/B)(E/100\,\mathrm{EeV})$, of UHECRs in Galactic magnetic fields is much larger than the thickness of the Galactic disk. Thus, confinement in the Galaxy is not maintained at the highest energies, motivating the search for extragalactic sources. Requiring that candidate sources be capable of confining particles up to E_{max} translates into a simple selection criterium for candidate sources with magnetic field strength B and extension R (Hillas 1984): $r_L \leq R$, i.e., $E \leq E_{max} \sim 1\,\mathrm{EeV}\,Z(B/1\,\mu\mathrm{G})(R/1\,\mathrm{kpc})$. **Figure 8** presents the so-called Hillas diagram, where candidate sources are placed in a B–R phase-space, taking into account the uncertainties on these parameters. Most astrophysical objects do not even reach

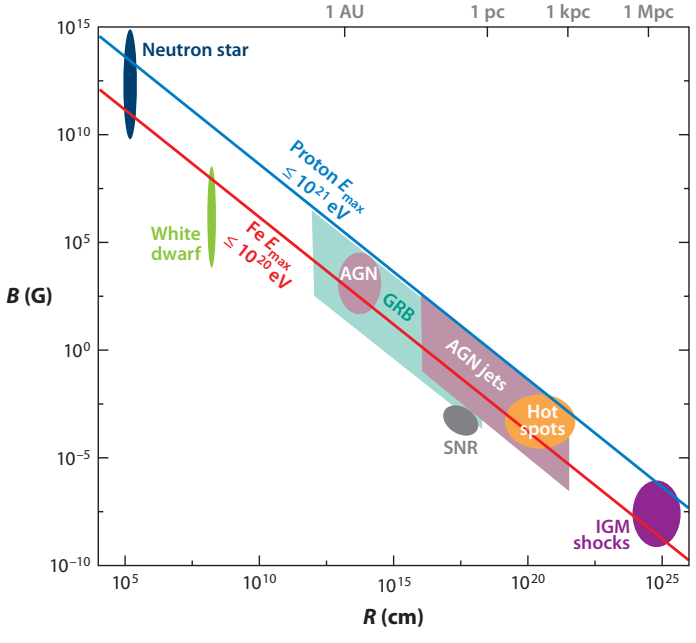

Figure 8

Updated Hillas (1984) diagram. Above the dark blue lines, protons can be confined to energies above $E_{max} = 10^{21}$ eV. Above the red line, iron nuclei can be confined to energies above $E_{max} = 10^{20}$ eV. The most powerful candidate sources are shown with the uncertainties in their parameters. Abbreviations: AGN, active galactic nuclei; GRB, gamma-ray burst; IGM, intergalactic medium; SNR, supernova remnant.

the iron confinement line up to 10^{20} eV, leaving the best candidates for UHECR acceleration to be neutron stars, AGN, GRBs, and accretion shocks in the IGM. The Hillas criterion is a necessary condition, but not sufficient. In particular, most UHECR acceleration models rely on time-dependent environments and relativistic outflows, where the Lorentz factor is $\Gamma \gg 1$. In the rest frame of the magnetized plasma, particles can only be accelerated over a transverse distance R/Γ, which subsequently changes the Hillas criterion.

The maximum accessible energy further depends on many details of the acceleration region, but can be estimated by comparing the acceleration time $t_{\rm acc}$, the escape time of particles from the acceleration region $t_{\rm esc}$, the lifetime of the source $t_{\rm age}$, and the energy-loss time due to expansion and to interactions with the ambient medium $t_{\rm loss}$ (see, e.g., Norman, Melrose & Achterberg 1995; Lemoine & Waxman 2009). The condition for successful acceleration can then be written $t_{\rm acc} \lesssim t_{\rm esc}, t_{\rm age}, t_{\rm loss}$. The escape timescale $t_{\rm esc} = R^2/(2D)$, where D is the diffusion coefficient, depends on the characteristics of the transport of particles in the ambient medium, i.e., on the magnetic field and on the turbulence features. Detailed studies of this subject can be found in, e.g., Jokipii (1966), Giacalone & Jokipii (1999), Casse, Lemoine & Pelletier (2002), Yan & Lazarian (2002), Candia & Roulet (2004), and Marcowith, Lemoine & Pelletier (2006). Energy losses during acceleration are generally due to synchrotron radiation, to interactions with the radiative backgrounds, or to hadronic interactions, the latter process being mostly inefficient in diluted astrophysical media. The timescale for energy losses through synchrotron emission and pion production can be expressed in a generic way (Biermann & Strittmatter 1987): $t_{\rm rad} = (6\pi m_p^4 c^3/\sigma_{\rm T} m_e^2) E^{-1} B^{-2} (1+A)^{-1}$, where $A = 240\, U_\gamma/U_B$ corresponds to the ratio of the energy density of radiation leading to pion production U_γ, to the magnetic energy density $U_B = B^2/8\pi$. In the central region of an AGN, for example, assuming equipartition with the magnetic field (corresponding to the Eddington luminosity), for $E_{20} = E/10^{20}$ eV and $B_{\rm G} = B/1$ G, $t_{\rm rad} \sim 10^5\,{\rm s}\, E_{20}^{-1} B_{\rm G}^{-2}$. This timescale has to be compared to the acceleration timescale, which reads (Lemoine & Waxman 2009) $t_{\rm acc} = \mathcal{A}\, t_{\rm L}$, where $t_{\rm L}$ is the Larmor timescale and $\mathcal{A} \gtrsim 1$ for all types of Fermi acceleration (non-, mildly, or ultrarelativistic first- and second-order Fermi accelerations). For a non-relativistic first-order Fermi acceleration, for instance, $\mathcal{A} \sim g/\beta_{\rm sh}^2$ and $t_{\rm acc} \sim 10^7\,{\rm s}\, g\, E_{20} B_{\rm G}^{-1} \beta_{\rm sh}^{-2}$, where the shock velocity $\beta_{\rm sh} \ll 1$ and $g \equiv D/(r_{\rm L} c) \gtrsim 1$. Majoring this timescale with the radiative-loss timescale leads to a maximum acceleration energy in the central region of AGN of order $E_{\rm max} \sim 10^{19}\,{\rm eV}\, g^{-1/2} B_{\rm G}^{-1/2} \beta_{\rm sh}$.

In the generic case of acceleration in an outflow, Lemoine & Waxman (2009) compare this acceleration time and the dynamical time, $t_{\rm dyn} \sim R/\beta_{\rm W}\Gamma_{\rm W} c$, of the outflow to set a robust lower bound on the luminosity that a source must possess in order to be able to accelerate particles up to $E = 10^{20}\,{\rm eV}\, E_{20} : L > L_B \equiv \Gamma_{\rm W} R^2 B^2/2 > 10^{45}\, Z^{-2} E_{20}^2\ {\rm erg\ s^{-1}}$. The magnetic luminosity L_B of the source is written as a function of the size of the acceleration region R in the observer frame, in motion with Lorentz factor $\Gamma_{\rm W}$ (and velocity $\beta_{\rm W}$) and imparted with a magnetic field of characteristic strength B. This quantity is not straightforward to derive: The classical determination of the field strength using the synchrotron emission (assuming equipartition between the total energy density of nonthermal particles and of the magnetic field, for example) depends notably on the hardly known ratio between the leptonic and hadronic accelerated particles (e.g., Beck & Krause 2005). In the case of blazars, for example, Celotti & Ghisellini (2008) discuss that their jets are not magnetically dominated and that FR I (Faranoff-Riley I) radio galaxies, TeV blazars, and BL Lac objects only possess magnetic luminosities of order $10^{42-44}\ {\rm erg\ s^{-1}}$.

It should be noted that the escape of particles from acceleration regions is an intricate issue that has been scarcely discussed in detail in the literature (note, however, the works of Norman, Melrose & Achterberg 1995; Mannheim, Protheroe & Rachen 2001; Rachen 2008; and Allard & Protheroe 2009). Mannheim, Protheroe & Rachen (2001) and Rachen (2008) argue that one

promising way to have high-energy particles leave the magnetized acceleration site would be the result of tranforming into neutrons. However, it is not obvious that such a scenario could produce a power-law spectrum; the shape of the spectrum depends on the evolution of the optical depth to photo-pion production (see, e.g., Waxman 2001).

In addition to being able to accelerate up to $E_{\rm max} > 200$ EeV, candidate UHECR accelerators should have luminosities that can account for the observed fluxes. A simple estimate of the required luminosity can be calculated assuming that all sources have the same injection spectral index s, a L_{19} steady luminosity in cosmic rays above $E_{19} \equiv 10^{19}$ eV, and that they are distributed homogeneously in the Universe with a density n_s. To account for the observed flux of UHECRs at E_{19}, the main quantity at play, $n_s L_{19}$, scale as $(E^3 {\rm d}N/{\rm d}E)_{E=E_{19}} \sim 10^{24}\,{\rm eV}^2\,{\rm m}^{-2}\,{\rm s}^{-1}\,{\rm sr}^{-1}(n_s/10^{-5}\,{\rm Mpc}^{-3})(L_{19}/10^{42}\,{\rm erg\,s}^{-1})$ for the case of $s = 2.3$ and $E_{\rm max} = 10^{20.5}$ eV. For reference, the number density of normal galaxies in the Universe today is of order 10^{-2} Mpc^{-3} (Blanton et al. 2003), and it drops to 10^{-9}–10^{-8} Mpc^{-3} for FR II (Faranoff-Riley II) type galaxies (Wall et al. 2005). For transient sources, this scaling can be translated into $(\dot{n}_s/10^{-9}\,{\rm Mpc}^{-3}\,{\rm years}^{-1})\,(E_{\rm tot,19}/3 \times 10^{53}\,{\rm ergs})$, where $\dot{n}_{\rm s}$ is the birth rate of the source and $E_{\rm tot,19}$ is the total injected energy in cosmic rays above E_{19}.

Below we discuss the main astrophysical sites where UHECRs may originate.

6.1.1. Gravitational accretion shocks. The accretion of dark matter and gas produces shocks around the largest structures of the Universe (clusters of galaxies, filaments, walls), where diffusive shock acceleration can happen. For clusters of galaxies, one can estimate the linear extension of the magnetized shock to ∼1–10 Mpc and the magnetic field intensity on both sides of the shock to ∼1 μG (see, e.g., the recent radio detection of synchrotron radiation from bow shocks in a merging cluster by van Weeren et al. 2010 that indicates the presence of microgauss-level magnetic fields far from the cluster center), which would allow particles to be confined up to $E \sim 10^{20}$ eV. Note, however, that the strength of the magnetic field upstream of the shock could actually be $\ll 1$ μG, as it was produced out of the weakly magnetized void; thus, shock acceleration can occur only if the magnetic field upstream can be strongly amplified (M. Lemoine and E. Zweibel, private communication, and see tentative amplification mechanisms by Schlickeiser & Shukla 2003 and Zweibel & Everett 2010). The detection of very high-energy gamma rays from these shocks would enable us to constrain these parameters. Clusters of galaxies have been considered as promising accelerators by various researchers: Norman, Melrose & Achterberg (1995); Kang, Ryu & Jones (1996); Kang, Rachen & Biermann (1997); Miniati et al. (2000); Ryu & Kang (2003); Inoue, Aharonian & Sugiyama (2005); Inoue et al. (2007); and Murase, Inoue & Nagataki (2008). Recently, Vannoni et al. (2009) performed a detailed time-dependent numerical calculation, including energy losses due to interactions of protons with radiative backgrounds, and demonstrated that, for realistic shock speeds of a few thousand kilometers per second and a background magnetic field close to 1 μG, the maximum energy achievable by protons cannot exceed a few times 10^{19} eV, due to radiative losses.

6.1.2. Active galactic nuclei. AGN are composed of an accretion disk around a central supermassive black hole and are sometimes associated with jets terminating in lobes (or hot spots) that can be detected in radio. These objects can be classified into two categories: radio quiet AGN with no prominent radio emission or jets and radio-loud objects presenting jets. Both categories could, in principle, accelerate particles in their nuclei: For a black hole of mass $M_{\rm bh} \sim 10^9\,M_\odot$, the equipartition magnetic field in the central region yields $B \sim 300$ G. Assuming the central region to be of order $R \sim 100$ AU, particles could be confined up to $E_{\rm max} \sim 150$ EeV and accelerated to $E \lesssim 10^{20}$ eV by electrostatic acceleration in the black hole magnetosphere (e.g., Boldt

& Ghosh 1999). This energy is hardly reached by particles in practice due to energy losses that they experience in this dense region (see above and Norman, Melrose & Achterberg 1995, Henri et al. 1999, and Rieger & Mannheim 2000). Radio-loud galaxies could also accelerate particles in their inner jets, where one possible mechanism at play could be shear acceleration (see end of Section 5.1 and, e.g., Rieger, Bosch-Ramon & Duffy 2007). The quantity $BR \sim 0.3$ Gpc for the jets of $M_{\rm bh} \sim 10^9\, M_\odot$, leading to $E_{\rm max} \sim 300$ EeV, but the acceleration is limited by photo-interactions and adiabatic losses making the escape of UHE particles nontrivial (Mannheim 1993). The most powerful radio galaxies (Faranoff-Riley II galaxies and their associated Flat Spectrum Radio Quasars, noted FR II and FSRQ) present hot spots and bow shocks formed at the termination of the jets by interaction with the IGM. For these regions, the same estimates for particle confinement energies as in jets can be found. For hot spots, shock acceleration and escape should be easier than in the jet (see, e.g., Rachen & Biermann 1993), but the acceleration in the bow shock is nontrivial (Berezhko 2008). UHECR acceleration in AGN should lead to particular signatures in the gamma-ray spectrum of these sources, through various emissions such as proton synchrotron, photo-hadronic interactions that induce pair cascades, muon synchrotron, etc. With more gamma-ray data on each source over a wide energy range (with, e.g., the Cherenkov Telescope Array, i.e., CTA), one could distinguish these hadronic signatures from leptonic acceleration signatures and probe the UHECR acceleration in AGN (Hinton & Hofmann 2009). As discussed above, Lemoine & Waxman (2009) point out that only FR II/FSRQ radio galaxies with magnetic luminosity $L_B \gtrsim 10^{45}$ erg s^{-1} (following the modeling of Celotti & Ghisellini 2008) meet the energetic requirements to accelerate particles to the highest energies. Under this assumption, one may argue that the local FR II galaxies are well known and do not seem to correlate with the arrival direction of the highest energy events. Possible reasons for this could be that the extragalactic magnetic fields are stronger than expected and/or that cosmic rays are heavy nuclei. AGN are often suggested as continuous emitters of UHECRs; however, transient events such as AGN flares more easily meet the UHECR acceleration requirements (Farrar & Gruzinov 2009). Other transient models for UHECR acceleration are discussed next.

6.1.3. Gamma-ray bursts. The explosion of a GRB leads to the formation of multiple shock regions, which are potential acceleration zones for UHECRs. The value of the magnetic field at these shocks is estimated to be of order $B \sim 10^6$ G at a distance of $R \sim 10^{12}$ cm from the center. These values are derived for internal shocks that happen before the ejected plasma reaches the ISM, assuming $B \sim 10^{12}$ G near the central engine (of size $R \sim 10$ km) and an evolution of $B \propto R^{-1}$. The wide green region presented in **Figure 8** stems from this dependency: Parameters can take different values at different times of the GRB explosion. These objects have been examined by various researchers as possible sources of UHECRs (Waxman 1995, 2001; Vietri 1995; Gialis & Pelletier 2003; Murase et al. 2006, 2008). These researchers invoke Fermi processes at external shocks (Vietri 1995), at mildly relativistic internal or reverse shocks (Waxman 1995, 2001; Murase et al. 2008), or second-order Fermi processes through multiple interactions with mildly relativistic internal shocks (Gialis & Pelletier 2003). Overall, models allow acceleration up to $\sim 10^{20}$ eV provided that some assumptions on the source parameters are verified (e.g., magnetic field strength, turbulence, etc.). The flux of gamma rays reaching the Earth from GRBs is generally comparable to the observed flux of UHECRs, implying a tight energetic requirement for GRBs to be the sources of UHECRs. With a GRB rate of ~ 0.3 Gpc^{-3} year^{-1} at $z = 0$, it can be calculated that the energy injected isotropically (regardless of beaming) in UHECRs is of order $E_{\rm UHECR} \gtrsim 10^{53}$ erg (Guetta & Piran 2007, Zitouni et al. 2008, Budnik et al. 2008). Note also that the transient nature of these objects could possibly explain the lack of powerful counterparts correlating with the arrival direction of the highest energy cosmic rays.

6.1.4. Neutron stars. Neutrons stars—young millisecond magnetars to be precise—easily fulfill the Hillas criterion and might prove to be very good candidate sources, though they are scarcely discussed in the literature. Magnetars are neutron stars with extremely strong surface dipole fields of order 10^{15} G (see Wood & Thompson 2004, Harding & Lai 2006, and Merghetti 2008 for reviews). Blasi, Epstein & Olinto (2000) studied the possibility that UHECRs are accelerated through unipolar induction in the relativistic winds for rapidly rotating magnetars, building up on previous constraints by Venkatesan, Miller & Olinto (1997). The maximum energy reached by particles injected by these objects is very promising (see Section 5.2). Arons (2003) further developed the model and found that only 5% of the extragalactic magnetar population needs to be fast-rotators to account for the observed UHECR energetics. Magnetars, as GRBs, are transient sources and should not be observed in coincidence with UHECR arrival directions. The possibility of injecting large proportions of heavy nuclei into an acceleration region may be more easily met by young neutron stars than alternative models, due to their iron-rich surface and early environment.

6.2. Cosmic Ray Astronomy at Ultrahigh Energies

One of the most puzzling facts concerning UHECRs is the absence of clear sources in the arrival directions of the highest energy events. Indeed, if sources are powerful astrophysical objects, one would expect to see a counterpart in the arrival direction at the highest observed energies. At trans-GZK energies, current upper limits on the strength of cosmic magnetic fields suggest that particles should not be deflected by more than a few degrees (unless they are heavy nuclei), thus some correlation should exist with the underlying baryonic matter.

As a result, many researchers have searched for correlations between existing data and astrophysical object catalogs. For example, Tinyakov & Tkachev (2001, 2002), Gorbunov et al. (2002), and Gorbunov & Troitsky (2005) found a correlation between HiRes event directions and BL Lac catalogs that has been much debated (Evans, Ferrer & Sarkar 2002; Evans et al. 2004; Tinyakov & Tkachev 2004). Stanev et al. (1995) noted an association between arrival directions of UHECRs and the supergalactic plane that was not confirmed by AGASA results (Takeda et al. 1998) and that seems to have reappeared in the Auger results (Stanev 2009). The latest correlation result concerns the highest energy events ($E > 55$ EeV) detected by the Auger Observatory and AGN within a distance of <75 Mpc (Abraham et al. 2007, 2008c; Abreu et al. 2010).

It must be underlined that the AGN correlating with the Auger events are mostly not very powerful Seyfert type galaxies and are, thus, not favored as accelerators of UHECRs. Hence, what should be retained from that correlation is that it brings to light the hint of an anisotropic distribution of events at the highest energy with 99% CL, its most reasonable interpretation then being that events trace the large-scale structures along which AGN are distributed. Another possible interpretation is that Auger may be observing in part the last scattering surface of UHECRs rather than their source population (Kotera & Lemoine 2008b). The possibility that this fake correlation effect could play a non-negligible role was shown numerically by Ryu, Das & Kang (2010).

Another explanation to the absence of counterparts in the arrival direction of UHECRs could also reside in the very nature of the sources. The delay induced by extragalactic magnetic fields of mean strength B and coherence length λ_B on particles of charge Z and energy E with respect to photons over a distance D reads (Alcock & Hatchett 1978):

$$\delta t \simeq 2.3 \times 10^2 \text{ year } Z^2 \left(\frac{D}{10\,\text{Mpc}}\right)^2 \left(\frac{\lambda_B}{0.1\,\text{Mpc}}\right) \left(\frac{E}{10^{20}\,\text{eV}}\right)^{-2} \left(\frac{B}{10^{-9}\,\text{G}}\right)^2. \quad (1)$$

For intergalactic magnetic fields of lower overall strength ($B \lesssim 10^{-12}$ G), this formula indicates that the time delay is shorter than a year over 100 Mpc. However, the crossing of one single

magnetized filament (size $\bar{r}_i$ and field strength B) can lead to a slight deflection that induces a time delay with respect to a straight line of order (Alcock & Hatchett 1978, Waxman & Miralda-Escudé 1996, Harari et al. 2002, Kotera & Lemoine 2008b): $\delta t_i \simeq 0.93 \times 10^3 \text{ year} \, (\bar{r}_i/2 \text{ Mpc})^2 (B_i/10^{-8} \text{ G})^2 (\lambda_i/0.1 \text{ Mpc}) (E/10^{20} \text{ eV})^{-2}$.

For transient sources like GRBs, neutron stars or AGN flares that have an activity timescale $\ll \delta t$, this delay is sufficient to erase any temporal coincidence between UHECRs and their progenitors (Vietri 1995, Waxman 1995). Because these bursts are fairly rare in our local Universe (where observed UHECRs originate), one only expects to see particles from a particular bursting source if their arrival times are spread out over $\sigma_t \gtrsim 10^3$ years at 10^{20} eV. This spread should be particularly increased in the presence of magnetized scattering centers between the source and the observer. Kotera & Lemoine (2008b) and Kalli, Lemoine & Kotera (2011) discuss that this effect could induce an artificially enhanced correlation of UHECR arrival directions with the foreground matter density, which could be measured to identify the transient nature of the sources.

As discussed in Section 2.3, UHECR sky anisotropies and their composition are tightly connected. In particular, if an anisotropy signal is measured above an energy $E_{\rm thr}$, assuming that it is produced by heavy nuclei of charge Z, one expects an anisotropy signal to be also present at energy $> E_{\rm thr}/Z$ due to the proton component, depending on the proton–to–heavy nuclei ratio q_p/q_Z injected at the source (Lemoine & Waxman 2009). The evaluation of the anisotropy signals at both high and low energies should thus place constraints on the ratio q_p/q_Z.

6.3. Multimessenger Approach

Secondary neutrinos and photons can be produced by UHECRs when they interact with ambient baryonic matter and radiation fields inside the source or during their propagation from source to Earth. These particles travel in geodesics unaffected by magnetic fields and bear valuable information on the birthplace of their progenitors. The quest for sources of UHECRs has thus long been associated with the detection of neutrinos and gamma rays that might pinpoint the position of the accelerators in the sky.

The detection of these particles is not straightforward however: First, the propagation of gamma rays with energy exceeding several teraelectronvolts is affected by their interaction with CMB and radio photons. These interactions lead to the production of high-energy electron and positron pairs, which in turn up-scatter CMB or radio photons by inverse Compton processes, initiating electromagnetic cascades. As a consequence, one does not expect to observe gamma rays of energy above ∼100 TeV from sources located beyond a horizon of a few megaparsecs (Wdowczyk, Tkaczyk & Wolfendale 1972; Protheroe 1986; Protheroe & Stanev 1993). Above EeV energies, photons can again propagate over large distances, depending on the radio background, and can reach observable levels above 10 EeV (Lee 1998). Secondary neutrinos are very useful because, unlike cosmic rays and photons, they are not absorbed by the cosmic backgrounds while propagating through the Universe. In particular, they provide unique access to observing sources at petaelectronvolt energies. However, their small interaction cross section makes it difficult to detect them on the Earth, requiring the construction of cubic kilometer detectors (see, e.g., Anchordoqui & Montaruli 2010).

Secondary neutrinos and gamma rays generated at UHECR sources have been investigated by a number of researchers (Szabo & Protheroe 1994; Rachen & Mészáros 1998; Waxman & Bahcall 1999; Mücke et al. 1999, 2000; Anchordoqui et al. 2008; Kachelrieß, Ostapchenko & Tomàs 2008; Ahlers, Anchordoqui & Sarkar 2009; Allard & Protheroe 2009; Mannheim, Protheroe & Rachen 2001), placing particular focus on emissions from AGN and transient sources such as GRBs. The case of cluster accretion shocks has been studied by Inoue et al. (2007) and Murase, Inoue &

Nagataki (2008), and transient sources have been examined in detail by Waxman & Bahcall (2000), Dai & Lu (2001), Dermer (2002), Murase et al. (2006, 2008), and Murase (2007) for GRBs and by Murase, Mészáros & Zhang (2009) for magnetars. The normalization and the very existence of these secondaries highly depend on assumptions about the opacity of the acceleration region and on the shape of the injection spectrum as well as on the phenomenological modeling of the acceleration. For instance, Waxman & Bahcall (1999) obtain an estimate for the cosmic neutrino flux, by comparing the neutrino luminosity to the observed cosmic ray luminosity, in the specific case where the proton photo-meson optical depth equals unity. When the source is optically thick, Allard & Protheroe (2009) demonstrate that cosmic rays are not accelerated to the highest energies, and neutrinos above $E \sim$ EeV are sharply suppressed.

The existence of secondaries from interactions during the propagation of cosmic rays is less uncertain, but it is also subject to large variations according to the injected spectral index, chemical composition, maximum acceleration energy, and source evolution history. The magnetic field in the source environment, especially in clusters of galaxies, can play an important role by confining the charged UHECRs and thus lead to increased interaction probabilities (Berezinsky, Blasi & Ptuskin 1997; Colafrancesco & Blasi 1998; Rordorf, Grasso & Dolag 2004; de Marco et al. 2006; Armengaud, Sigl & Miniati 2006; Murase, Inoue & Nagataki 2008; Wolfe et al. 2008; Kotera et al. 2009).

A number of researchers have estimated the cosmogenic neutrino flux with varying assumptions (e.g., Engel, Seckel & Stanev 2001; Ave et al. 2005; Hooper, Taylor & Sarkar 2005; Seckel & Stanev 2005; Allard et al. 2006; Berezinsky 2006; Stanev et al. 2006; Takami et al. 2009; Kotera, Allard & Olinto 2010). **Figure 9** summarizes the effects of different assumptions about the UHECR source evolution, the Galactic to extragalactic transition, the injected chemical composition, and $E_{\rm max}$, on the cosmogenic neutrino flux. It demonstrates that the parameter space is currently poorly constrained with uncertainties of several orders of magnitude in the predicted flux. UHECR models with large proton $E_{\rm max}$ (>100 EeV), source evolution corresponding to the star-formation history or the GRB rate evolution, dip or ankle transition models, and pure proton or mixed Galactic compositions are shaded in gray in **Figure 9** and give detectable fluxes in the EeV range with 0.06–0.2 neutrino per year at IceCube and 0.03–0.06 neutrino per year for the Auger Observatory. If EeV neutrinos are detected, petaelectronvolt information can help select between competing models of cosmic ray composition at the highest energy and the Galactic to extragalactic transition at ankle energies. With improved sensitivity, zetaelectronvolt ($= 10^{21}$ eV) neutrino observatories, such as ANITA and JEM-EUSO, could explore the maximum acceleration energy.

The detectability of photons from the electromagnetic cascade triggered by pion production interactions has been addressed by several groups (e.g., Lee 1998; Ferrigno, Blasi & de Marco 2004; Armengaud, Sigl & Miniati 2006; Gelmini, Kalashev & Semikoz 2007; Kotera, Allard & Lemoine 2011). The dilution of the cascaded signal—due to the deflection of the electrons and positrons generated during the cascade—depends on the assumptions made regarding the configuration of the EGMF. More specifically, the gamma-ray flux scales as the fraction of the line of sight in which the magnetic field is smaller than the value B_θ such that the deflection of the low-energy cascade is θ (Kotera, Allard & Lemoine 2011). For reference, $B_\theta \simeq 2 \times 10^{-14}$ G for $\theta = 1°$, and one can refer to **Figure 7** for values of this fraction in different magnetic field configurations. Even under optimistic assumptions on the magnetic field configuration, only sources with extremely high luminosities $L_{E,19} \gtrsim 3 \times 10^{44}$ erg s^{-1} $(d/100\,{\rm Mpc})^{-2}$ and $L_{E,19} \gtrsim 10^{43}$ erg s^{-1} $(d/100\,{\rm Mpc})^{-2}$ for $E > 10^{19}$ eV could be detected by current instruments such as HESS and by the future CTA, respectively, with fluxes of order $\sim 10^{-10}$ GeV cm^{-2} s^{-1} around 1–10 TeV (Ferrigno, Blasi & de Marco 2004; Kotera, Allard & Lemoine 2011).

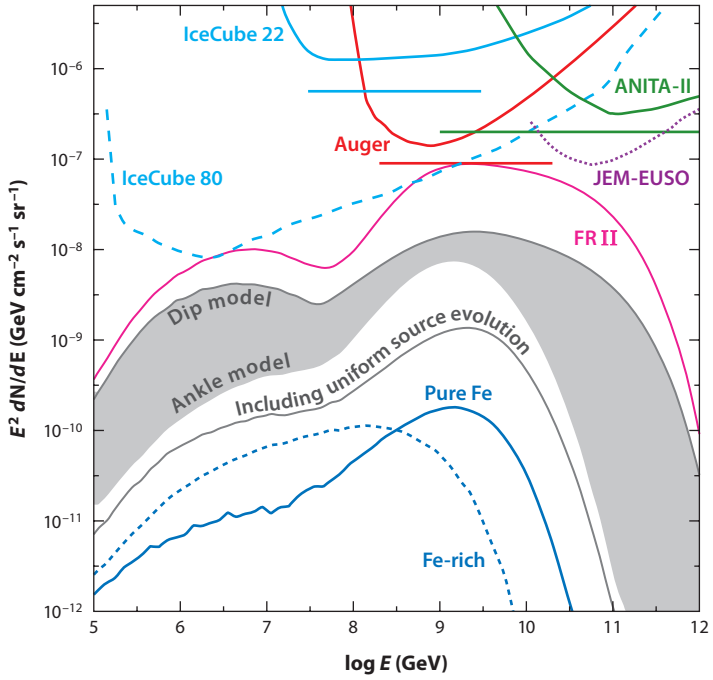

Figure 9

Cosmogenic neutrino flux for all flavors, for different ultrahigh-energy cosmic ray parameters compared to instrument sensitivities. Pink solid line corresponds to a strong source evolution case (FR II evolution; see Wall et al. 2005) with a pure proton composition, dip transition model, and $E_{\max} = 3$ ZeV. Dashed and solid dark blue lines correspond to uniform source evolution with: iron rich (30%) composition and $E_{Z,\max} < Z$ 10 EeV (*dotted line*) and pure iron injection and $E_{Z,\max} = Z$ 100 EeV (*solid*). Gray-shaded range brackets dip and ankle transition models, with evolution of star-formation history for $z < 4$, pure proton and mixed Galactic compositions, and large proton $E_{\max}$ (>100 EeV). Including the uniform source evolution would broaden the shaded area down to the gray solid line. Current experimental limits (*solid lines*) assume 90% confidence level and full mixing neutrino oscillation. The differential limit and the integral flux limit on a pure E^{-2} spectrum (*straight red line*) are presented for IceCube 22 lines (*pale blue*, Abbasi et al. 2010), ANITA-II (*green*, Gorham et al. 2010) and Auger South (*red*, Abraham et al. 2009b). For future instruments, we present the projected instrument sensitivities for IceCube 80 lines (*pale blue long dashed line*, acceptances from S. Yoshida, private communication; see also Karle 2010), and for JEM-EUSO (*purple dotted line*, Medina-Tanco et al. 2009).

Gabici & Aharonian (2005, 2007) argued that one should rather search for the gigaelectronvolt photons emitted by the synchrotron radiation of the secondary electrons in the presence of substantial magnetic fields in the source environment. Again, only the cases of rare powerful sources with cosmic ray luminosity $L_{E,19} > 10^{44-46}$ erg s^{-1} are promising in terms of detectability with both current and upcoming instruments. A source with a cosmic ray luminosity of $L_{E,19} \sim 10^{44}$ erg s^{-1} located at a distance $d \sim 100$ Mpc nearly overshoots the observed cosmic ray spectrum and is thus marginally excluded. Farther sources, with higher luminosity (e.g., $L_{E,19} = 10^{46}$ erg s^{-1} at $d = 1$ Gpc) would thus be more promising to observe in gamma rays. Such distant sources would contribute to about 10% of the observed spectrum of UHECRs up to $E \sim 10^{19}$ eV, and the cosmic rays produced with higher energy would not reach the Earth due to energy losses.

Finally, sources located at a distance $\lesssim$10 Mpc accelerating UHECRs should produce ultrahigh-energy photons during their propagation, which can reach the Earth before experiencing Compton cascading. Taylor et al. (2009) studied this potential signature in the

particular case of our closest radio galaxy Cen A (3.8 Mpc) and concluded that Auger should be able to detect 0.05–0.075 photon per year from Cen A, assuming that it is responsible for 10% of the cosmic ray flux above 60 EeV and assuming a 25% efficiency for photon discrimination.

One last messenger that is scarcely discussed in relation to UHECRs is gravitational waves. If anisotropy signals reveal that the source is of transient type, one way to establish whether UHECR sources are GRBs or magnetars would be to look for gravitational waves produced by the latter, as the former are believed to produce only faint signals below detectability (e.g., Piran 2004). Kotera (2011, arXiv:1106.3060) shows that the distribution of magnetar initial voltages required to reconcile the produced spectrum to the observed one should lead to higher stochastic gravitational wave signals from these objects than previously calculated (e.g., Regimbau & Mandic 2008). The observation of such a gravitational wave signal could be a probe that these objects meet the requirements (in terms of magnetization, rotation velocity, and inertial momentum) to accelerate UHECRs to the highest energies.

It should be highlighted that due to the delay induced by EGMF on charged cosmic rays (see Section 6.2), secondary neutrinos, photons, and gravitational waves should not be detected in time coincidence with UHECRs if the sources are not continuously emitting particles, but are transient such as GRBs and young magnetars.

7. THE SEARCH FOR ULTRAHIGH-ENERGY COSMIC RAY SOURCES

The resolution of the long-standing mystery of the origin of UHECRs will require a coordinated approach on three complementary fronts: the direct UHECR frontier, the transition region between the knee and the ankle, and the multimessenger interface with high-energy photons and neutrinos.

The most direct route to a resolution of this open question would be a precise measurement of the three pillars of UHECR observations: spectrum, anisotropies, and composition. The spectrum is much better measured today than just a few years ago and will certainly improve in the years to come with current observatories. The precise shape and energy scale of the ankle and the cutoff are excellent selectors of models. For instance, a possible recovery at the highest energies can clearly show the GZK nature of the cutoff as opposed to a cutoff caused by the maximum acceleration energy. A precise energy scale for the ankle will test a propagation dip versus a Galactic to extragalactic cosmic ray transition.

More discriminating than the precise shape of the spectrum, but much harder to plan for success, is a clear observation of anisotropies. A nearby source, the first UHECR source, will clearly be a watershed in the field. A clear correlation with the large-scale structure within 200 Mpc will also clear the path to zeroing in at the possible accelerators.

The most difficult but key observable of the three pillars is a clear composition measurement. The dependence on hadronic models to translate shower properties into composition measurements makes it difficult to reach definitive conclusions. Progress in this arena can be done at the transition region between the knee and the ankle, where the LHC has direct access to the energy scale. Enlarging the range of cosmic ray measurements to higher energies from the knee (KASCADE-Grande) and to lower energies from the ankle (Auger HEAT and AMIGA, and TALE) will help construct a unified model of the cosmic ray properties in a region that hadronic models can be tested at the LHC (see **http://www-ik.fzk.de/~needs/** for a list of measurements that can be made at accelerator programs to improve the ability of hadronic models to interpret cosmic ray observables).

A clear anisotropy determination, especially above 60 EeV, will help determine the composition astrophysically. At these energies, possible composition mixtures simplify tremendously for sources

above tens of megaparsecs into two options: protons or iron-like. Iron-like nuclei will have much broader spread in arrival directions due to known magnetic fields erasing small-scale anisotropies and opening the possibility of a clear signature of proton primaries for some anisotropic patterns. An astrophysically determined primary composition will open a fruitful avenue to compare interaction models with observed shower properties at energies orders of magnitude above the reach of laboratory accelerators.

The spectrum and composition between the knee and the ankle should signal the transition from Galactic to extragalactic cosmic rays. A clear observation of a second knee or composition studies around the ankle can produce clear signatures of the transition. Anisotropies are not expected at these energies unless neutrons manage to escape Galactic acceleration sites. Progress in this energy range will also come from direct gamma-ray observations of cosmic accelerators (e.g., by Fermi, CTA, and the High Altitude Water Cherenkov Experiment, or HAWC) and their deeper understanding. Neutrinos in this energy range can also be crucial if sources can be identified or if cosmogenic neutrinos are observed in the petaelectronvolt range (e.g., IceCube, KM3NeT).

Observations of photons and neutrinos at ultrahigh energies will be extremely useful in distinguishing proposed scenarios (e.g., by IceCube, Auger, JEM-EUSO, and ANITA). Photons will only reach us from nearby accelerators, so they can be directly connected to acceleration sites. Neutrinos may be observed from nearby sources or from the diffuse background expected from the propagation of UHECRs from cosmologically distant objects. Having both a nearby view of the apparently brightest accelerators as well as the integrated flux from more distant objects will strongly constrain possible candidates.

As an exercise, we end by contrasting two of the many possible outcomes of future observations. In outcome A, the large-scale structure correlation is confirmed above the 5-σ level showing that UHECR sources exist within the GZK sphere and that their sky position is not smeared by more than a few degrees. These observations will imply that: (*a*) UHECR sources are more common than clusters of galaxies or powerful blazars, and (*b*) the composition above 60 EeV should be dominated by protons. If shower properties continue to show a trend toward iron-like behavior, it is likely to be due to changes in hadronic interactions, given that at 60 EeV only iron or protons arrive from sources further than tens of megaparsecs. This scenario is rich with multimessengers: Ultrahigh-energy photons from nearby sources and neutrinos from sources and the diffuse background should be observable. The type of galaxies that UHECR events correlate with may signal an origin in active galaxies, encouraging models based on central supermassive black holes. If starburst galaxies correlate better, magnetars and GRBs would be better candidate sources. Protons above 60 EeV do not prevent a mixed composition at EeV, so measurements of the composition at the ankle will help determine the injected composition and source spectral index.

In a second case B, above 60 EeV the spectrum does not show a recovery, anisotropies are not observed even after a significant increase in statistics, and shower properties indicate iron-like primaries. In this case, the maximum energy of the accelerators is likely to be below GZK energies for protons, and the spectrum cutoff is likely to be a combined effect of the maximum iron energy and the GZK effect. This coincidence is not an elegant solution, but it is a clear possibility. A heavy composition at injection is more natural for models based on magnetars, whereas scenarios based on AGN and GRBs need to be modified to account for the suprisingly heavy composition. In this scenario, cosmogenic neutrinos and photons will not be easily detected, leaving only the hope of observing a nearby source or of major technological advances to reach down orders of magnitude in flux.

Great progress in the UHECR frontier may lead to a completely different outcome than our speculative exercise above, but that will require a significant increase in statistics at trans-GZK energies. Current data suggest that watershed anisotropies will only become clear above 60 EeV

and that very large statistics with good angular and energy resolution will be required. Auger will add $7 \times 10^3 L$ per year in the South, whereas TA will add about $2 \times 10^3 L$ per year in the North. Current technologies can reach a goal of another order of magnitude if deployed by bold scientists over very large areas (e.g., Auger North). New technologies may ease the need for large numbers of detector units to cover similarly large areas. Future space observatories (e.g., JEM-EUSO, OWL, Super-EUSO) promise a new avenue to reach the necessary high statistics, especially if improved photon detection technologies are achieved. With a coordinated effort, the next generation of observatories can explore more of the ~5 million trans-GZK events the Earth's atmosphere receives per year.

DISCLOSURE STATEMENT

The authors are not aware of any affiliations, memberships, funding, or financial holdings that might be perceived as affecting the objectivity of this review.

ACKNOWLEDGMENTS

We thank Denis Allard, Venya Berezinsky, Peter Biermann, Klaus Dolag, Ralph Engel, Susumu Inoue, Hyesung Kang, Martin Lemoine, Chris McKee, Teresa Montaruli, Sterl Phinney, Dongsu Ryu, Dmitri Semikoz, Todor Stanev, and Ellen Zweibel for very helpful input to this manuscript. We thank the Auger collaboration for the brilliant work at the subject's frontier. This work was supported by NSF grant PHY-0758017 at the University of Chicago, and the Kavli Institute for Cosmological Physics through grant NSF PHY-0551142 and an endowment from the Kavli Foundation.

LITERATURE CITED

Abbasi RU, Abu-Zayyad T, Allen M, Amann JF, Archbold G, et al. 2008a. *Ap. J.* 684:790
Abbasi RU, Abu-Zayyad T, Allen M, Amann JF, Archbold G, et al. 2008b. *Phys. Rev. Lett.* 100:101101
Abbasi RU, Abu-Zayyad T, Allen M, Amann JF, Archbold G, et al. 2008c. *Astropart. Phys.* 30:175
Abbasi RU, Abu-Zayyad T, Al-Seady M, Allen M, Amann JF, et al. (High Resolut. Fly's Eye Collab.) 2009. *Astropart. Phys.* 32:53
Abbasi RU, Abu-Zayyad T, Al-Seady M, Allen M, Amann JF, et al. 2010. *Phys. Rev. Lett.* 104:161101
Abbasi RU, Abu-Zayyad T, Amann JF, Archbold G, Bellido JA, et al. (High Resolut. Fly's Eye Collab.) 2004. *Phys. Rev. Lett.* 92:151101
Abraham J, Abreu P, Aglietta M, Aguirre C, Ahn EJ, et al. 2009a. *Proc. 31st Int. Cosm. Ray Conf., Lodz, Pol.*
Abraham J, Abreu P, Aglietta M, Aguirre C, Allard D, et al. 2008a. *Phys. Rev. Lett.* 101:061101
Abraham J, Abreu P, Aglietta M, Ahn EJ, Allard D, et al. 2010a. *Phys. Rev. Lett.* 104:091101
Abraham J, Abreu P, Aglietta M, Ahn EJ, Allard D, et al. 2010b. *Phys. Lett. B* 685:239
Abraham J, Creusot A, Ferry S, Filipčič A, Horvat M, et al. 2007. *Science* 318:938
Abraham J, Creusot A, Ferry S, Filipčič A, Horvat M, et al. 2008b. *Astropart. Phys.* 29:243
Abraham J, Creusot A, Ferry S, Filipčič A, Horvat M, et al. 2008c. *Astropart. Phys.* 29:188
Abraham J, Creusot A, Filipčič A, Horvat M, Verberič D, et al. 2004. *Nucl. Instrum. Methods Phys. Res. A* 523:50
Abraham J, Creusot A, Filipčič A, Hussain M, Verberič D, et al. 2009b. *Phys. Rev. D* 79:102001
Abraham J, Creusot A, Filipčič A, Hussain M, Verberič D, et al. 2009c. *Astropart. Phys.* 31:399
Abreu P, Aglietta M, Ahn EJ, Allard D, Allekotte I, et al. 2010. *Astropart. Phys.* 34:314
Aguirre A, Hernquist L, Schaye J, Weinberg DH, Katz N, Gardner J. 2001. *Ap. J.* 560:599
Aharonian FA, Kelner SR, Prosekin AY. 2010. *Phys. Rev. D* 82:043002
Ahlers M, Anchordoqui LA, Sarkar S. 2009. *Phys. Rev. D* 79:083009

Ahn HS, Adams JH, Bashindzhagyan G, Batkov KE, Chang J, et al. 2008. In *Int. Cosm. Ray Conf.*, ed. R Caballero, JC D'Olivo, G Medina-Tanco, L Nellen, FA Sánchez, JF Valdés-Galicia, 2:79. Univ. Nac. Autón Méx., Mex. City
Ahn HS, Allison PS, Bagliesi MG, Barbier L, Beatty JJ, et al. 2010. *Ap. J.* 714:L89
Alcock C, Hatchett S. 1978. *Ap. J.* 222:456
Allard D, Ave M, Busca N, Malkan MA, Olinto AV, et al. 2006. *J. Cosmol. Astropart. Phys.* 9:5
Allard D, Busca NG, Decerprit G, Olinto AV, Parizot E. 2008. *J. Cosmol. Astropart. Phys.* 10:33
Allard D, Parizot E, Olinto AV. 2007. *Astropart. Phys.* 27:61
Allard D, Parizot E, Olinto AV, Khan E, Goriely S. 2005. *Astron. Astrophys.* 443:L29
Allard D, Protheroe RJ. 2009. *Astron. Astrophys.* 502:803
Aloisio R, Berezinsky VS. 2005. *Ap. J.* 625:249
Aloisio R, Berezinsky VS, Gazizov A. 2011. *Astropart. Phys.* 34:620–26
Alvarez-Muñiz J, Engel R, Stanev T. 2002. *Ap. J.* 572:185
Amato E, Blasi P. 2005. *MNRAS* 364:L76
Amato E, Blasi P. 2006. *MNRAS* 371:1251
Amato E, Blasi P. 2009. *MNRAS* 392:1591
Amenomori M, Bi XJ, Chen D, Cui SW, Danzengluobu, et al. [Tibet ASγ Collab.] 2008. *Ap. J.* 678:1165–79
Anchordoqui LA, Hooper D, Sarkar S, Taylor AM. 2008. *Astropart. Phys.* 29:1
Anchordoqui LA, Montaruli T. 2010. *Annu. Rev. Nucl. Part. Sci.* 60:129
Apanasenko AV, Beresovskaya VA, Fujii M, Galkin VI, Hareyama M. 2001. In *Proc. 27th Int. Cosm. Ray Conf.*, *Hamburg, Ger.*, p. 1622
Apel WD, Arteaga JC, Badea F, Bekk K, Bertaina M, et al. 2009. *Proc. 31st Int. Cosm. Ray Conf.*, *Lodz, Pol.* (arXiv 0906.4007)
Armengaud E, Sigl G, Beau T, Miniati F. 2007. *Astropart. Phys.* 28:463
Armengaud E, Sigl G, Miniati F. 2006. *Phys. Rev. D* 73:083008
Arons J. 2003. *Ap. J.* 589:871
Ave M, Busca N, Olinto AV, Watson AA, Yamamoto T. 2005. *Astropart. Phys.* 23:19
Axford WI, Leer E, Skadron G. 1977. In *Proc. 15th Int. Cosm. Ray Conf.*, *Plovdiv* 11:132
Baltrusaitis R, Cady R, Cassiday G, Cooperv R, Elbert JW, et al. 1985. *Nucl. Instr. Methods A* 240:410
Beatty JJ, Westerhoff S. 2009. *Annu. Rev. Nucl. Part. Sci.* 59:319
Beck R. 2008. In *AIP Conf. Proc.* 1085:83
Beck R, Gaensler B, Feretti L. 2007. *SKA and the Magnetic Universe*, pp. 103. Berlin: Springer-Verlag
Beck R, Krause M. 2005. *Astron. Nachr.* 326:414
Bednarz J, Ostrowski M. 1998. *Phys. Rev. Lett.* 80:3911
Begelman MC, Rudak B, Sikora M. 1990. *Ap. J.* 362:38
Bell AR. 1978. *MNRAS* 182:147
Bell AR. 2004. *MNRAS* 353:550
Bell AR, Lucek SG. 2001. *MNRAS* 321:433
Berezhko EG. 2008. *Ap. J. Lett.* 684:L69
Berezhko EG, Ellison DC. 1999. *Ap. J.* 526:385
Berezinsky V. 2006. *Nucl. Phys. B Proc. Suppl.* 151:260
Berezinsky V, Gazizov AZ, Grigorieva SI. 2005. *Phys. Lett. B* 612:147
Berezinsky V, Gazizov AZ, Grigorieva SI. 2006. *Phys. Rev. D* 74:043005
Berezinsky VS, Blasi P, Ptuskin VS. 1997. *Ap. J.* 487:529
Berezinsky VS, Bulanov SV, Dogiel VA, Ginzburg VL, Ptuskin VS. 1990. In *Astrophysics of Cosmic Rays*, Chapter 4, ed. VL Ginzburg. Amsterdam: North Holland
Berezinsky VS, Gazizov AZ. 1993. *Phys. Rev. D* 47:4206
Berezinsky VS, Grigorieva SI. 1988. *Astron. Astrophys.* 199:1
Bertone G, Isola C, Lemoine M, Sigl G. 2002. *Phys. Rev. D* 66:103003
Bertone S, Stoehr F, White SDM. 2005. *MNRAS* 359:1201
Bertone S, Vogt C, Enßlin T. 2006. *MNRAS* 370:319
Bhattacharjee A, Sigl G. 2000. *Phys. Rep.* 327:109
Biermann PL, Cassinelli JP. 1993. *Astron. Astrophys.* 277:691

Biermann PL, Strittmatter PA. 1987. *Ap. J.* 322:643
Bird DJ, Corbato SC, Dai HY, Dawson BR, Elbert JW, et al. 1994. *Ap. J.* 424:491
Birk GT, Wiechen H, Lesch H, Kronberg PP. 2000. *Astron. Astrophys.* 353:108
Blandford RD, Ostriker JP. 1978. *Ap. J. Lett.* 221:L29
Blanton MR, Hogg DW, Bahcall NA, Brinkman J, Britton M, et al. 2003. *Ap. J.* 592:819
Blasi P, Burles S, Olinto AV. 1999. *Ap. J. Lett.* 514:L79
Blasi P, Epstein RI, Olinto AV. 2000. *Ap. J. Lett.* 533:L123
Blasi P, Olinto AV. 1999. *Phys. Rev. D* 59:023001
Bluemer J, Engel R, Hoerandel JR. 2009. *Prog. Part. Nucl. Phys.* 63:293
Boldt E, Ghosh P. 1999. *MNRAS* 307:491
Boyer JH, Knapp BC, Mannel EJ, Seman M. 2002. *Nucl. Instrum. Methods Phys. Res. A* 482:457
Brüggen M, Ruszkowski M, Simionescu A, Hoeft M, Dalla Vecchia C. 2005. *Ap. J. Lett.* 631:L21
Bruni M, Maartens R, Tsagas CG. 2003. *MNRAS* 338:785
Buckley R. 1977. *Nature* 266:37
Budnik R, Katz B, MacFadyen A, Waxman E. 2008. *Ap. J.* 673:928
Calvez A, Kusenko A, Nagataki S. 2010. *Phys. Rev. Lett.* 105:091101
Candia J, Roulet E. 2004. *J. Cosmol. Astropart. Phys.* 10:7
Casse F, Lemoine M, Pelletier G. 2002. *Phys. Rev. D* 65:023002
Celotti A, Ghisellini G. 2008. *MNRAS* 385:283
Cen R, Nagamine K, Ostriker JP. 2005. *Ap. J.* 635:86
Chen P, Tajima T, Takahashi Y. 2002. *Phys. Rev. Lett.* 89:161101
Chiba N, Dion GM, Hayashida N, Honda K, Honda M, et al. 1992. *Astropart. Phys.* 1:27
Colafrancesco S, Blasi P. 1998. *Astropart. Phys.* 9:227
Contopoulos I, Kazanas D. 2002. *Ap. J.* 566:336
Coroniti FV. 1990. *Ap. J.* 349:538
Cronin JW. 2005. *Nucl. Phys. B Proc. Suppl.* 138:465
Dai ZG, Lu T. 2001. *Ap. J.* 551:249
Das S, Kang H, Ryu D, Cho J. 2008. *Ap. J.* 682:29
de Gouveia Dal Pino EM, Lazarian A. 2000. *Ap. J. Lett.* 536:L31
de Gouveia Dal Pino EM, Lazarian A. 2005. *Astron. Astrophys.* 441:845
de Marco D, Hansen P, Stanev T, Blasi P. 2006. *Phys. Rev. D* 73:043004
Dermer CD. 2002. *Ap. J.* 574:65
Dieckmann ME, Shukla PK, Drury LOC. 2008. *Ap. J.* 675:586
Dolag K, Grasso D, Springel V, Tkachev I. 2004. *J. Korean Astron. Soc.* 37:427
Dolag K, Grasso D, Springel V, Tkachev I. 2005. *J. Cosmol. Astropart. Phys.* 1:9
Donnert J, Dolag K, Lesch H, Müller E. 2009. *MNRAS* 392:1008
Dubois Y, Teyssier R. 2008. *Astron. Astrophys.* 482:L13
Engel R, Seckel D, Stanev T. 2001. *Phys. Rev. D* 64:093010
Epele LN, Roulet E. 1998a. *Phys. Rev. Lett.* 81:3295
Epele LN, Roulet E. 1998b. *J. High Energy Phys.* 10:9
Evans NW, Ferrer F, Sarkar S. 2002. *Astropart. Phys.* 17:319
Evans NW, Ferrer F, Sarkar S. 2004. *Phys. Rev. D* 69:128302
Farrar GR, Gruzinov A. 2009. *Ap. J.* 693:329
Fermi E. 1949. *Phys. Rev.* 75:1169
Ferrigno C, Blasi P, de Marco D. 2004. *Nucl. Phys. B Proc. Suppl.* 136:191
Gabici S, Aharonian FA. 2005. *Phys. Rev. Lett.* 95:251102
Gabici S, Aharonian FA. 2007. *Ap. J. Lett.* 665:L131
Gaisser TK. 1991. *Cosmic Rays and Particle Physics*. New York: Cambridge Univ. Press
Gallant YA, Achterberg A. 1999. *MNRAS* 305:L6
Gelmini G, Kalashev O, Semikoz DV. 2007. *Astropart. Phys.* 28:390
Genzel H, Joos P, Pfiel W, eds. 1973. *Photoproduction of Elementary Particles. Numerical Data and Functional Relationships in Science and Technology*, Vol. 8. Berlin: Springer-Verlag
George MR, Fabian AC, Baumgartner WH, Mushotzky RF, Tueller J. 2008. *MNRAS* 388:L59

Giacalone J, Jokipii JR. 1999. *Ap. J.* 520:204
Gialis D, Pelletier G. 2003. *Astropart. Phys.* 20:323
Gialis D, Pelletier G. 2004. *Astron. Astrophys.* 425:395
Gialis D, Pelletier G. 2005. *Ap. J.* 627:868
Giannios D. 2010. *MNRAS* 408:L46
Globus N, Allard D, Parizot E. 2008. *Astron. Astrophys.* 479:97
Gorbunov DS, Tinyakov PG, Tkachev II, Troitsky SV. 2002. *Ap. J. Lett.* 577:L93
Gorbunov DS, Troitsky SV. 2005. *Astropart. Phys.* 23:175
Gorham PW, Allison P, Baughman BM, Beatty JJ, Belov K, et al. 2010. *Phys. Rev. D* 82:022004
Greisen K. 1966. *Phys. Rev. Lett.* 16:748
Grigorov NL, Gubin YV, Rapoport ID, Savenko IA, Yakovlev BM. 1971. *Proc. 12th Int. Cosm. Ray Conf., Hobart, Aust.* 5:1746
Gruzinov A, Waxman E. 1999. *Ap. J.* 511:852
Guetta D, Piran T. 2007. *J. Cosmol. Astropart. Phys.* 7:3
Han JL. 2008. *Nucl. Phys. B Proc. Suppl.* 175:62
Han JL, Manchester RN, Lyne AG, Qiao GJ, van Straten W. 2006. *Ap. J.* 642:868
Han JL, Manchester RN, Qiao GJ. 1999. *MNRAS* 306:371
Harari D, Mollerach S, Roulet E. 1999. *J. High Energy Phys.* 8:22
Harari D, Mollerach S, Roulet E. 2002a. *J. High Energy Phys.* 7:6
Harari D, Mollerach S, Roulet E. 2006. *J. Cosmol. Astropart. Phys.* 11:12
Harari D, Mollerach S, Roulet E, Sánchez F. 2002b. *J. High Energy Phys.* 3:45
Harding AK, Lai D. 2006. *Rep. Progr. Phys.* 69:2631
Hededal CB, Nishikawa K. 2005. *Ap. J. Lett.* 623:L89
Henri G, Pelletier G, Petrucci PO, Renaud N. 1999. *Astropart. Phys.* 11:347
Hillas AM. 1984. *Annu. Rev. Astron. Astrophys.* 22:425
Hillas AM. 2006. In *Proc. Cosmol. Galaxy Form. Astropart. Phys. Pathw. SKA*, ed. H-R Klöckner, M Jarvis, S Rawlings. April 10–12, p. 9. Oxford, UK (astro-ph/0607109)
Hinton JA, Hofmann W. 2009. *Annu. Rev. Astron. Astrophys.* 47:523
Hooper D, Sarkar S, Taylor AM. 2008. *Phys. Rev. D* 77:103007
Hooper D, Taylor A, Sarkar S. 2005. *Astropart. Phys.* 23:11
Hooper D, Taylor AM. 2010. *Astropart. Phys.* 33:151
Huchra JP, Martimbeau N, Jarrett T, Cutri R, Skrutskie M, et al. 2005. *IAU Symp.* 216:170
Ide Y, Nagataki S, Tsubaki S, Yoshiguchi H, Sato K. 2001. *Publ. Astron. Soc. Jpn.* 53:1153
Inoue S, Aharonian FA, Sugiyama N. 2005. *Ap. J. Lett.* 628:L9
Inoue S, Sigl G, Miniati F, Armengaud E. 2007. *Proc. 30th Int. Cosm. Ray Conf., Merida, Mex.*
Isola C, Lemoine M, Sigl G. 2002. *Phys. Rev. D* 65:023004
Isola C, Sigl G. 2002. *Phys. Rev. D* 66:083002
Jansson R, Farrar GR, Waelkens AH, Ensslin TA. 2009. *J. Cosmol. Astropart. Phys.* 2009(07):21
Jokipii JR. 1966. *Ap. J.* 146:480
Kachelrieß M, Ostapchenko S, Tomàs R. 2008. *Phys. Rev. D* 77:023007
Kachelrieß M, Semikoz DV. 2006. *Phys. Lett. B* 634:14
Kachelrieß M, Serpico PD, Teshima M. 2007. *Astropart. Phys.* 26:378
Kalli S, Lemoine M, Kotera K. 2011. *Astron. Astrophys.* 528:109
Kampert K-H, Antoni T, Apel WD, Badea F, Bekk K, et al. 2004. *Nucl. Phys. B Proc. Suppl.* 136:273
Kang H, Rachen JP, Biermann PL. 1997. *MNRAS* 286:257
Kang H, Ryu D, Jones TW. 1996. *Ap. J.* 456:422
Karle A. 2010. *Proc. 31st Int. Cosm. Ray Conf., Lodz, Pol.*, 2009 (arXiv 1003.5715)
Kashti T, Waxman E. 2008. *J. Cosmol. Astropart. Phys.* 5:6
Khan E, Goriely S, Allard D, Parizot E, Suomijarvi T, et al. 2005. *Astropart. Phys.* 23:191
King EJ, Coles P. 2006. *MNRAS* 365:1288
Kirk JG, Guthmann AW, Gallant YA, Achterberg A. 2000. *Ap. J.* 542:235
Kneiske TM, Bretz T, Mannheim K, Hartmann DH. 2004. *Astron. Astrophys.* 413:807
Kotera K, Allard D, Lemoine M. 2011. *Astron. Astrophys.* In press

Kotera K, Allard D, Murase K, Aoi J, Dubois Y, et al. 2009. *Ap. J.* 707:370
Kotera K, Allard D, Olinto AV. 2010. *J. Cosmol. Astropart. Phys.* 10:13
Kotera K, Lemoine M. 2008a. *Phys. Rev. D* 77:023005
Kotera K, Lemoine M. 2008b. *Phys. Rev. D* 77:123003
Kronberg PP. 1994. *Rep. Progr. Phys.* 57:325
Kronberg PP, Lesch H, Hopp U. 1999. *Ap. J.* 511:56
Kulsrud RM, Zweibel EG. 2008. *Rep. Progr. Phys.* 71:046901
Lagage PO, Cesarsky CJ. 1983. *Astron. Astrophys.* 125:249
Lee S. 1998. *Phys. Rev. D* 58:043004
Lemoine M. 2005. *Phys. Rev. D* 71:083007
Lemoine M, Pelletier G. 2003. *Ap. J. Lett.* 589:L73
Lemoine M, Pelletier G, Revenu B. 2006. *Ap. J. Lett.* 645:L129
Lemoine M, Sigl G, Olinto AV, Schramm DN. 1997. *Ap. J. Lett.* 486:L115+
Lemoine M, Waxman E. 2009. *J. Cosmol. Astropart. Phys.* 0911:009
Letessier-Selvon A, Stanev T. 2011. *Rev. Mod. Phys.* In press
Linsley J. 1963. *Phys. Rev. Lett.* 10:146
Lucek SG, Bell AR. 2000. *MNRAS* 314:65
Lyubarsky Y, Kirk JG. 2001. *Ap. J.* 547:437
Lyubarsky YE. 2003. *MNRAS* 345:153
Lyutikov M, Ouyed R. 2007. *Astropart. Phys.* 27:473
Malkov MA, O'C Drury L. 2001. *Rep. Progr. Phys.* 64:429
Mannheim K. 1993. *Astron. Astrophys.* 269:67
Mannheim K, Protheroe RJ, Rachen JP. 2001. *Phys. Rev. D* 63:023003
Marcowith A, Lemoine M, Pelletier G. 2006. *Astron. Astrophys.* 453:193
Maximon L. 1968. *J. Res. Nat. Bur. Stand. B* 72:79
McKenzie JF, Voelk HJ. 1982. *Astron. Astrophys.* 116:191
Medina-Tanco G, Asano K, Cline D, Ebisuzaki T, Inoue S, et al. 2009. *Proc. 31st Int. Cosm. Ray Conf., Lodz, Pol.* (arXiv 0909.3766v1)
Medina-Tanco GA. 1998. *Ap. J. Lett.* 505:L79
Medina-Tanco GA, de Gouveia Dal Pino EM, Horvath JE. 1997. *Astropart. Phys.* 6:337
Medvedev MV, Loeb A. 1999. *Ap. J.* 526:697
Medvedev MV, Zakutnyaya OV. 2009. *Ap. J.* 696:2269
Mereghetti S. 2008. *Astron. Astrophys. Rev.* 15:225
Milosavljević M, Nakar E. 2006. *Ap. J.* 641:978
Miniati F, Ryu D, Kang H, Jones TW, Cen T, Ostriker JP. 2000. *Ap. J.* 542:608
Miralda-Escudé J, Waxman E. 1996. *Ap. J. Lett.* 462:L59+
Mücke A, Engel R, Rachen JP, Protheroe RJ, Stanev T. 2000. *Comput. Phys. Commun.* 124:290
Mücke A, Rachen JP, Engel R, Protheroe RJ, Stanev T. 1999. *Publ. Astron. Soc. Aust.* 16:160
Murase K. 2007. *Phys. Rev. D* 76:123001
Murase K, Inoue S, Nagataki S. 2008a. *Ap. J. Lett.* 689:L105
Murase K, Ioka K. 2008. *Ap. J.* 676:1123
Murase K, Ioka K, Nagataki S, Nakamura T. 2006. *Ap. J. Lett.* 651:L5
Murase K, Ioka K, Nagataki S, Nakamura T. 2008b. *Phys. Rev. D* 78:023005
Murase K, Mészáros P, Zhang B. 2009. *Phys. Rev. D* 79:103001
Nagano M, Watson AA. 2000. *Rev. Mod. Phys.* 72:689
Neronov A, Semikoz DV. 2009. *Phys. Rev. D* 80:123012
Neronov A, Semikoz DV, Tinyakov PG, Tkachev II. 2011. *Astron. Astrophys.* 526:A90
Neronov A, Vovk I. 2010. *Science* 328:73
Niemiec J, Ostrowski M, Pohl M. 2006. *Ap. J.* 650:1020
Nonaka T, Abu-Zayyad T, Allen M, Azuma R, Belz JW, et al. 2009. *Nucl. Phys. Proc. Suppl.* 190:26
Norman CA, Melrose DB, Achterberg A. 1995. *Ap. J.* 454:60
Olinto AV. 2000. *Phys. Rep.* 333:329
Pelletier G. 1999. *Astron. Astrophys.* 350:705

Pelletier G, Kersalé E. 2000. *Astron. Astrophys.* 361:788
Pelletier G, Lemoine M, Marcowith A. 2009. *MNRAS* 393:587
Piran T. 2004. *Rev. Mod. Phys.* 76:1143
Protheroe RJ. 1986. *MNRAS* 221:769
Protheroe RJ, Stanev T. 1993. *MNRAS* 264:191
Ptuskin V, Zirakashvili V, Seo E-S. 2010. *Ap. J.* 718:31
Puget JL, Stecker FW, Bredekamp JH. 1976. *Ap. J.* 205:638
Rachen JP. 2008. In *Proc. XXth Rencontres de Blois*, "Challenges in Particle Astrophysics," ed. J Dumarchez, JT Thanh Van, pp. 287–90. Hanoi, Vietnam: The Gioi (arXiv 0808.0349)
Rachen JP, Biermann PL. 1993. *Astron. Astrophys.* 272:161
Rachen JP, Mészáros P. 1998. *Phys. Rev. D* 58:123005
Regimbau T, Mandic V. 2008. *Class. Quantum Gravity* 25:184018
Reville B, Kirk JG, Duffy P, O'Sullivan S. 2007. *Astron. Astrophys.* 475:435
Reville B, O'Sullivan S, Duffy P, Kirk JG. 2008. *MNRAS* 386:509
Rieger FM, Bosch-Ramon V, Duffy P. 2007. *Astrophys. Space Sci.* 309:119
Rieger FM, Duffy P. 2005. *Ap. J. Lett.* 632:L21
Rieger FM, Mannheim K. 2000. *Astron. Astrophys.* 353:473
Riquelme MA, Spitkovsky A. 2010. *Ap. J.* 717:1054
Rordorf C, Grasso D, Dolag K. 2004. *Astropart. Phys.* 22:167
Ryu D, Das S, Kang H. 2010. *Ap. J.* 710:1422
Ryu D, Kang H. 2003. *J. Korean Astron. Soc.* 36:105
Ryu D, Kang H, Biermann PL. 1998. *Astron. Astrophys.* 335:19
Ryu D, Kang H, Cho J, Das S. 2008. *Science* 320:909
Scannapieco E, Pichon C, Aracil B, Petitjean P, Thacker RJ, et al. 2006. *MNRAS* 365:615
Schlickeiser R, Shukla PK. 2003. *Ap. J. Lett.* 599:L57
Schwarzschild B. 2010. *Phys. Today* 63N5:15
Seckel D, Stanev T. 2005. *Phys. Rev. Lett.* 95:141101
Shapiro SL, Teukolsky SA. 1983. *Black Holes, White Dwarfs, and Neutron Stars: The Physics of Compact Objects.* New York: Wiley
Siemieniec-Oziebło G, Golda ZA. 2004. *Astron. Astrophys.* 422:23
Sigl G, Lemoine M, Biermann P. 1999. *Astropart. Phys.* 10:141
Sigl G, Lemoine M, Olinto AV. 1997. *Phys. Rev. D* 56:4470
Sigl G, Miniati F, Enßlin TA. 2004. *Phys. Rev. D* 70:043007
Silva LO, Fonseca RA, Tonge JW, Dawson JM, Mori WB, Medvedev MV. 2003. *Ap. J. Lett.* 596:L121
Spitkovsky A. 2008. *Ap. J. Lett.* 682:L5
Stanev T. 2009. *Proc. Workshop Vulcano 2008*, ed. F Giovanelli, G Mannocchi. Soc. Ital. Fisica, Bologna, p. 609 (arXiv 0808.1236v1)
Stanev T. 2010. *High Energy Cosmic Rays*. Chichester, UK: Praxis
Stanev T, Biermann PL, Lloyd-Evans J, Rachen JP, Watson A. 1995. *Phys. Rev. Lett.* 75:3056
Stanev T, de Marco D, Malkan MA, Stecker FW. 2006. *Phys. Rev. D* 73:043003
Stanev T, Seckel D, Engel R. 2003. *Phys. Rev. D* 68:103004
Stecker FW. 1968. *The production of cosmic gamma-rays in interstellar and intergalactic cosmic-ray collisions*. PhD thesis. Harvard Univ.
Stecker FW, Malkan MA, Scully ST. 2006. *Ap. J.* 648:774
Stecker FW, Salamon MH. 1999. *Ap. J.* 512:521
Szabo AP, Protheroe RJ. 1994. *Astropart. Phys.* 2:375
Tajima T, Dawson JM. 1979. *Phys. Rev. Lett.* 43:267
Takami H, Murase K, Nagataki S, Sato K. 2009. *Astropart. Phys.* 31:201
Takami H, Sato K. 2008. *Ap. J.* 681:1279
Takami H, Yoshiguchi H, Sato K. 2006. *Ap. J.* 639:803
Takeda M, Hayashida N, Honda K, Inoue N, Kadota K, et al. 1998. *Phys. Rev. Lett.* 81:1163
Taylor AM, Hinton JA, Blasi P, Ave M. 2009. *Phys. Rev. Lett.* 103:051102
Thompson C. 2006. *Ap. J.* 651:333

Tinyakov PG, Tkachev II. 2001. *JETP Lett.* 74:1
Tinyakov PG, Tkachev II. 2002. *Astropart. Phys.* 18:165
Tinyakov PG, Tkachev II. 2004. *Phys. Rev. D* 69:128301
Tinyakov PG, Tkachev II. 2005. *Astropart. Phys.* 24:32
Tokuno H, Abu-Zayyad T, Aida R, Allen M, Azuma R, et al. 2009. *Nucl. Instrum. Methods A* 601:364
Tueller J, Baumgartner WH, Markwardt CB, Skinner GK, Mushotzky RF, et al. 2010. *Ap. J. Suppl.* 186:378
Vallée JP. 2004. *New Astron. Rev.* 48:763
Vannoni G, Aharonian FA, Gabici S, Kelner SR, Prosekin A. 2011. *Astron. Astrophys.* In press
van Weeren RJ, Röttgering HJA, Brüggen M, Hoeft M. 2010. *Science* 330:347
Venkatesan A, Miller MC, Olinto AV. 1997. *Ap. J.* 484:323
Véron-Cetty M-P, Véron P. 2006. *Astron. Astrophys.* 455:773
Vietri M. 1995. *Ap. J.* 453:883
Wall JV, Jackson CA, Shaver PA, Hook IM, Kellermann KI. 2005. *Astron. Astrophys.* 434:133
Waxman E. 1995. *Phys. Rev. Lett.* 75:386
Waxman E. 2001. In *Phys. Astrophys. Ultra-High Energy Cosm. Rays*, *Lect. Notes Phys.*, ed. M Lemoine, G Sigl, 576:122. Berlin: Springer-Verlag
Waxman E, Bahcall J. 1999. *Phys. Rev. D* 59:023002
Waxman E, Bahcall JN. 2000. *Ap. J.* 541:707
Waxman E, Miralda-Escudé J. 1996. *Ap. J. Lett.* 472:L89+
Wdowczyk J, Tkaczyk W, Wolfendale AW. 1972. *J. Phys. A Math. Gen.* 5:1419
Wdowczyk J, Wolfendale AW. 1979. *Nature* 281:356
Wibig T, Wolfendale AW. 2005. *J. Phys. G* 31:255
Widrow LM. 2002. *Rev. Mod. Phys.* 74:775
Wolfe B, Melia F, Crocker RM, Volkas RR. 2008. *Ap. J.* 687:193
Woods PM, Thompson C. 2006. In *Compact Stellar X-ray Sources*, ed. W Lewin, M van der Klis, Cambridge Astrophys. Ser. 39, pp. 547–86. Cambridge, UK: Cambridge Univ. Press
Yan H, Lazarian A. 2002. *Phys. Rev. Lett.* 89:281102
Zatsepin G, Kuzmin V. 1966. *J. Exp. Theor. Phys. Lett.* 4:78
Zirakashvili VN, Ptuskin VS, Völk HJ. 2008. *Ap. J.* 678:255
Zitouni H, Daigne F, Mochkovich R, Zerguini TH. 2008. *MNRAS* 386:1597
Zweibel EG, Everett JE. 2010. *Ap. J.* 709:1412
Zweibel EG, Yamada M. 2009. *Annu. Rev. Astron. Astrophys.* 47:291

Annual Review of Astronomy and Astrophysics

Volume 49, 2011

Contents